# Decision Support Framework for Optimal Reservoir Operation to Mitigate Cyanobacterial Blooms in Rivers

Kim, Jongchan; Jonoski, Andreja; Solomatine, Dimitri P.; Goethals, Peter L. M.

**DOI**
10.3390/su151712789

**Publication date**
2023

**Document Version**
Final published version

**Published in**
Sustainability

**Citation (APA)**
Kim, J., Jonoski, A., Solomatine, D. P., & Goethals, P. L. M. (2023). Decision Support Framework for Optimal Reservoir Operation to Mitigate Cyanobacterial Blooms in Rivers. *Sustainability*, *15*(17), Article 12789. https://doi.org/10.3390/su151712789

*sustainability*

MDPI

*Article*

# Decision Support Framework for Optimal Reservoir Operation to Mitigate Cyanobacterial Blooms in Rivers

**Jongchan Kim [1,2,3,*], Andreja Jonoski [1], Dimitri P. Solomatine [1,3] and Peter L. M. Goethals [4]**

[1] Department of Hydroinformatics and Socio-Technical Innovation, IHE Delft Institute for Water Education, 2611 AX Delft, The Netherlands; a.jonoski@un-ihe.org (A.J.); d.solomatine@un-ihe.org (D.P.S.)
[2] K-water, Daejeon 34350, Republic of Korea
[3] Water Resources Section, Delft University of Technology, 2628 CD Delft, The Netherlands
[4] Department of Animal Sciences and Aquatic Ecology, Ghent University, 9000 Ghent, Belgium; peter.goethals@ugent.be
* Correspondence: j.kim-3@tudelft.nl

**Abstract:** Flow control flushing water from reservoirs has been imposed in South Korea for mitigating harmful cyanobacterial blooms (CyanoHABs) in rivers. This measure, however, can cause water shortage in reservoirs, as the measure adopting this flow control may require an additional amount of water which exceeds the water demand allocated to the reservoirs. In terms of sustainability, a trade-off between improving water quality and alleviating water shortage needs to be considered. This study aimed at establishing a practical framework for a decision support system for optimal joint operation of the upstream reservoirs (Andong and Imha) to reduce the frequency of CyanoHABs in the Nakdong River, South Korea. Methodologically, three models were introduced: (1) a machine learning model (accuracy 88%) based on the k-NN (k-Nearest Neighbor) algorithm to predict the occurrence of CyanoHABs at a selected downstream location (the Chilgok Weir located approximately 140 km downstream from the Andong Dam), (2) a multiobjective optimization model employing NSGA-II (Nondominated Sorting Genetic Algorithm II) to determine both the quantity and quality of water released from the reservoirs, and (3) a river water quality model ($R^2$ 0.79) using HEC-RAS to simulate the water quality parameter at Chilgok Weir according to given upstream boundary conditions. The applicability of the framework was demonstrated by simulation results using observational data from 2015 to 2019. The simulation results based on the framework confirmed that the frequency of CyanoHABs would be decreased compared with the number of days when CyanoHABs were observed at Chilgok Weir. This framework, with a combination of several models, is a novelty in terms of efficiency, and it can be a part of a solution to the problem of CyanoHABs without using an additional amount of water from a reservoir.

**Keywords:** harmful cyanobacterial blooms; reservoir operation; framework; machine learning model; optimization model; river water quality model; nitrate nitrogen



**Citation:** Kim, J.; Jonoski, A.; Solomatine, D.P.; Goethals, P.L.M. Decision Support Framework for Optimal Reservoir Operation to Mitigate Cyanobacterial Blooms in Rivers. *Sustainability* **2023**, *15*, 12789. https://doi.org/10.3390/su151712789

Academic Editor: Mike Spiliotis

Received: 10 July 2023
Revised: 11 August 2023
Accepted: 22 August 2023
Published: 24 August 2023



## 1. Introduction

As the amount of water resources in reservoirs is limited, such water resources need to be efficiently used considering the different perspectives of stakeholders. Reservoir operation agencies typically prioritize the exploitation of water resources based on quantity. Conversely, environmental organizations can advocate for reservoirs to be operated with a focus on enhancing water quality. Both viewpoints are essential for the sustainability of both human and natural systems. While ensuring an adequate water supply reduces the risk of shortages, improving water quality positively impacts aquatic ecosystems and public health. Nevertheless, achieving improved water quality in rivers through reservoir operations necessitates significant water discharge from reservoirs. This can give rise to a potential conflict between stakeholders concerned with water quantity in reservoirs and those prioritizing water quality in rivers. In order to address these conflicting demands

and promote sustainable development, optimal reservoir operations must simultaneously consider both the quantity and quality of water.

Reservoir operations have been mainly focused on the management of water quantity, such as water supply, hydropower generation, and flood control [1,2]. However, recent studies have aimed at improving water quality downstream through the efficient operation of reservoirs [2–4]. Water quality downstream can be improved by discharging more clean water from a reservoir, but this reservoir operation may also cause an increase in the risk of water shortages.

Harmful cyanobacterial blooms (CyanoHABs; abbreviations used in this study are shown in Appendix A) appear when phytoplankton exponentially increase in lentic water bodies with low flow velocities such as lakes and reservoirs due to eutrophication [5–10]. In South Korea, CyanoHABs, which negatively impact water quality, have been an environmental problem in rivers, particularly since 2012 [7,11,12], when the Korean government constructed 16 weirs in the middle of rivers within the Four Major Rivers Restoration Project [12]. This project has raised a matter of controversy with the problem of water quality. This is because of the claim that the weirs have caused the frequent occurrence of CyanoHABs in the rivers, where the flow velocity has decreased [12]. According to the Ministry of Environment in South Korea, BOD (Biochemical Oxygen Demand) and TP (Total Phosphorus), which are the main parameters of water quality to be managed in rivers, at major points of the four rivers as of 2021, were measured as follows: BOD 1.6 mg $L^{-1}$ and TP 0.074 mg $L^{-1}$ at the point Noryangjin of the Han River, BOD 2.2 mg $L^{-1}$ and TP 0.037 mg $L^{-1}$ at the point Waegwan of the Nakdong River, BOD 2.4 mg $L^{-1}$ and TP 0.054 mg $L^{-1}$ at the point Buyeo1 of the Geum River, and BOD 5.3 mg $L^{-1}$ and TP 0.169 mg $L^{-1}$ at the point Naju of the Yeongsan River [13].

CyanoHABs can produce toxic substances, such as microcystins [14–16]. Human health may be damaged through the ingestion of water containing these toxic substances [14–16] or the inhalation of aerosolized cyanotoxins [17,18]. Thus, the management of water quality is of paramount importance in terms of preventing the occurrence of CyanoHABs. To effectively mitigate CyanoHABs, predicting the incidence of CyanoHABs is required. However, the prediction of the occurrence of CyanoHABs is challenging due to the complexity of factors involved, such as climate, water quality, flow conditions, and chemical and biological processes [19].

To tackle this issue concerning CyanoHABs, many studies have covered the model-based prediction of harmful algae blooms. According to Rousso et al. [19], forecasting and predictive models for CyanoHABs were developed in various forms depending on modeling techniques. Previous studies concerned data-driven models based on techniques such as artificial neural networks, decision trees, and Bayesian networks, as well as process-based models such as DYRESM-CAEDYM, ELCOM-CAEDYM, and WASP [19]. In addition, research on not only methodologies of modeling harmful algal blooms in consideration of climate change [20] but also a web-based modeling framework for harmful algal blooms simulation [21] was conducted. These studies, however, did not focus on preventing the occurrence of CyanoHABs but on predicting their occurrence. If these studies are designed to link with a practical method for reducing the frequency of CyanoHABs, viable strategies can be proposed to effectively control CyanoHABs.

In South Korea, reservoir operation for mitigating CyanoHABs has primarily focused on flow control flushing water from a reservoir to a river downstream [22,23]. However, the use of water in reservoirs for improving water quality has not been generally factored into the design of reservoirs in South Korea [24–26]. Hence, the flow control using an additional amount of water has been only temporarily taken in order to mitigate CyanoHABs [22], since this flow control can cause water shortage. For a trade-off between the conflicting objectives of improving water quality and alleviating water shortage, optimal operation of reservoirs must be conducted by simultaneously considering both the quantity and quality of water.

A selective withdrawal facility (SWF) is designed and used for controlling the quality of water released from a reservoir [27–30]. In South Korea, the Imha Reservoir [31,32] and the Soyanggang Reservoir [27,33] are equipped with an SWF. Previous studies have demonstrated the effectiveness of SWFs regarding the exclusion of turbid water from reservoirs, which is the primary purpose of SWFs [31–33]. As SWFs enable the selection of water quality by depth, they can control not only the water quality of the reservoir upstream but also downstream. Therefore, SWFs are a critical factor for the optimal operation of reservoirs considering the improvement of water quality downstream.

However, there have been few studies on reservoir operation using SWFs in terms of addressing issues about biological parameters of water quality, such as CyanoHABs in a downstream river. Previous studies [2–4] have not focused on CyanoHABs but on physical or chemical parameters, such as temperature, DO (Dissolved Oxygen), and $PO_4$ (Phosphate). This can be because simulating biological parameters of water quality is more complex compared with physical or chemical parameters.

The main objective of this study is to establish a practical framework for a decision support system aimed at decreasing the frequency of occurrence of CyanoHABs at Chilgok Weir based on the optimal joint operation of two upstream reservoirs (Andong and Imha reservoirs). The two reservoirs and the Chilgok Weir are located in the Nakdong River of South Korea. Methodologically, we first present a framework of a decision support system. Secondly, three models are presented for this framework. These models include a machine learning model based on the k-NN (k-Nearest Neighbor) algorithm for predicting the occurrence of CyanoHABs at Chilgok Weir, an optimization model employing NSGA-II (Nondominated Sorting Genetic Algorithm II) for the joint operation of the two reservoirs considering both the quantity and quality of water, and a river water quality model using HEC-RAS to link the machine learning and optimization models. Finally, the applicability of this framework is demonstrated using observational data and the three models in terms of reducing the frequency of occurrence of CyanoHABs at Chilgok Weir.

Demonstrating the effectiveness of the framework incorporating water quality modeling and the optimization process of reservoir operation can provide a feasible solution to the problem of the incidence of CyanoHABs in rivers. To the best of our knowledge, this is the first study to focus on mitigating CyanoHABs in rivers based on the optimal operations of reservoirs.

## 2. Materials and Methods

### *2.1. Study Area*

The Nakdong River is one of the major rivers in South Korea, measuring approximately 510 km in length and serving as a water source for surrounding regions [34] while being vulnerable to pollutants because of a lot of agricultural activities [35]. In the Nakdong River basin, there are ten multipurpose dams and eight weirs, as shown in Figure 1. We selected the upper reach of the Nakdong River as a study area, covering the Andong Reservoir, the Imha Reservoir, and the Chilgok Weir. The Andong Reservoir is situated furthest upstream, while the Imha Reservoir is located in the Banbyeoncheon River, a tributary of the Nakdong River. The Andong and Imha reservoirs have effective storage volumes of 1000 million $m^3$ and 424 million $m^3$, respectively, with catchment areas of 1584 $km^2$ and 1361 $km^2$, respectively [36]. The Chilgok Weir is located approximately 140 km downstream away from the Andong Dam.

There are three principal reasons for the selection of this study area. First, a joint operation can be conducted for the two reservoirs, Andong and Imha. This joint operation makes the amount of the water supply from each reservoir flexible in conditions of meeting the sum of water demand of both reservoirs. Secondly, the Imha Reservoir is equipped with an SWF [31,32], which enables the control of the quality of water released to the downstream river. Finally, the Chilgok Weir is close to the intake facilities for drinking water [37], making the management of water quality at Chilgok Weir a critical issue. A

monitoring station for water quality data, including cyanobacterial cell density, is located 500 m upstream of the Chilgok Weir [7].

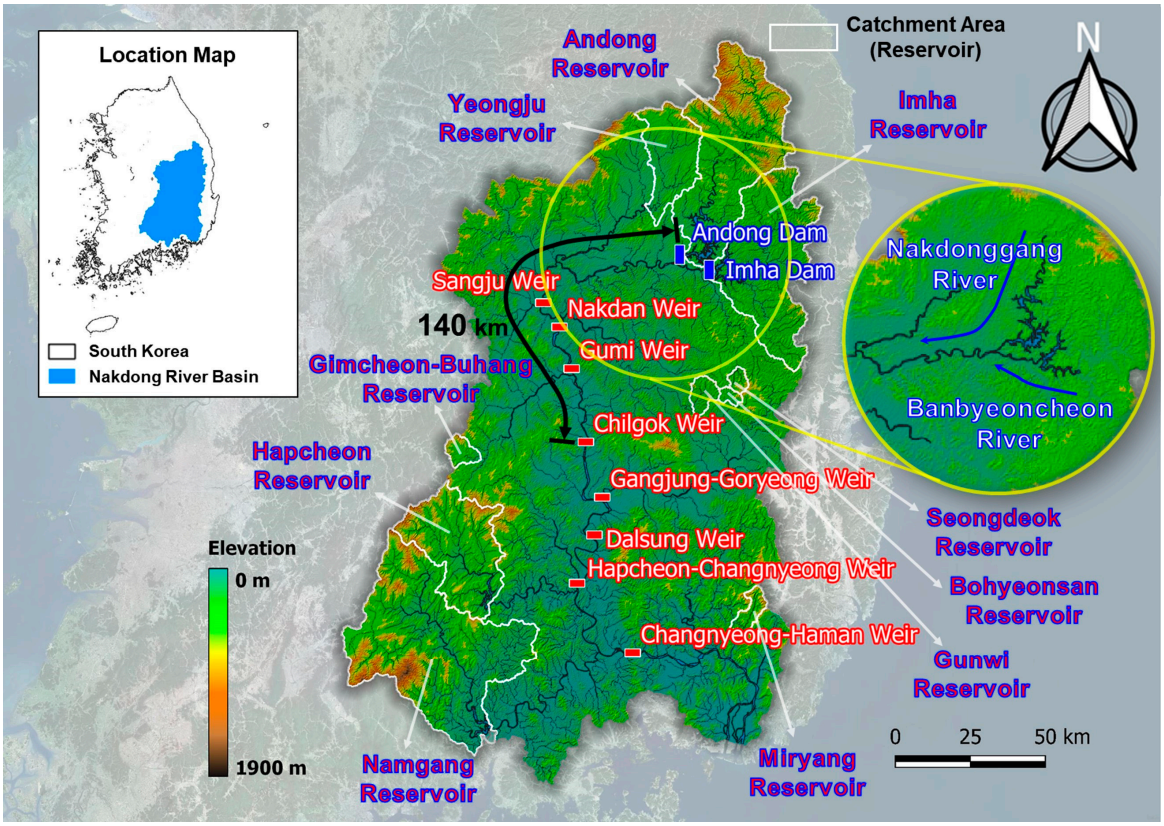


**Figure 1.** Location and schematization of the study area.

### *2.2. Framework for Decision Support System*

We established a framework for a decision support system to reduce the incidence of CyanoHABs at Chilgok Weir through an optimal joint operation of the upstream reservoirs (Andong and Imha reservoirs), as shown in Figure 2. The framework comprises six steps, as follows:

1. Step 1 applies a machine learning model to predict the occurrence or the nonoccurrence of CyanoHABs at Chilgok Weir using observational data, which are input features associated with CyanoHABs. The forecast horizon of the machine learning model is one week.
2. In the event of a prediction of the occurrence of CyanoHABs one week ahead (Step 1), the water quality of the Andong and Imha reservoirs is simulated by their depths in Step 2. The water quality parameters of this simulation are consistent with the input features of the machine learning model of Step 1.
3. Step 3 involves an optimization process in which the decision variables include the quantity of water released from both reservoirs and the quality of water from the Imha Reservoir. The objective functions and constraints of this optimization are aimed at decreasing the frequency of CyanoHABs at Chilgok Weir and satisfying the water demand downstream.
4. In Step 4, the water quality at Chilgok Weir is simulated using a river water quality model by incorporating the optimization results from Step 3 as upstream boundary conditions.
5. Step 5 is a process for confirming whether CyanoHABs would not occur after one week at Chilgok Weir, based on the water quality simulated in Step 4 by applying the machine learning model of Step 1.

6. If the prediction result from Step 5 indicates that CyanoHABs would not occur at Chilgok Weir, the Andong and Imha reservoirs will finally be operated using the optimization results from Step 3.

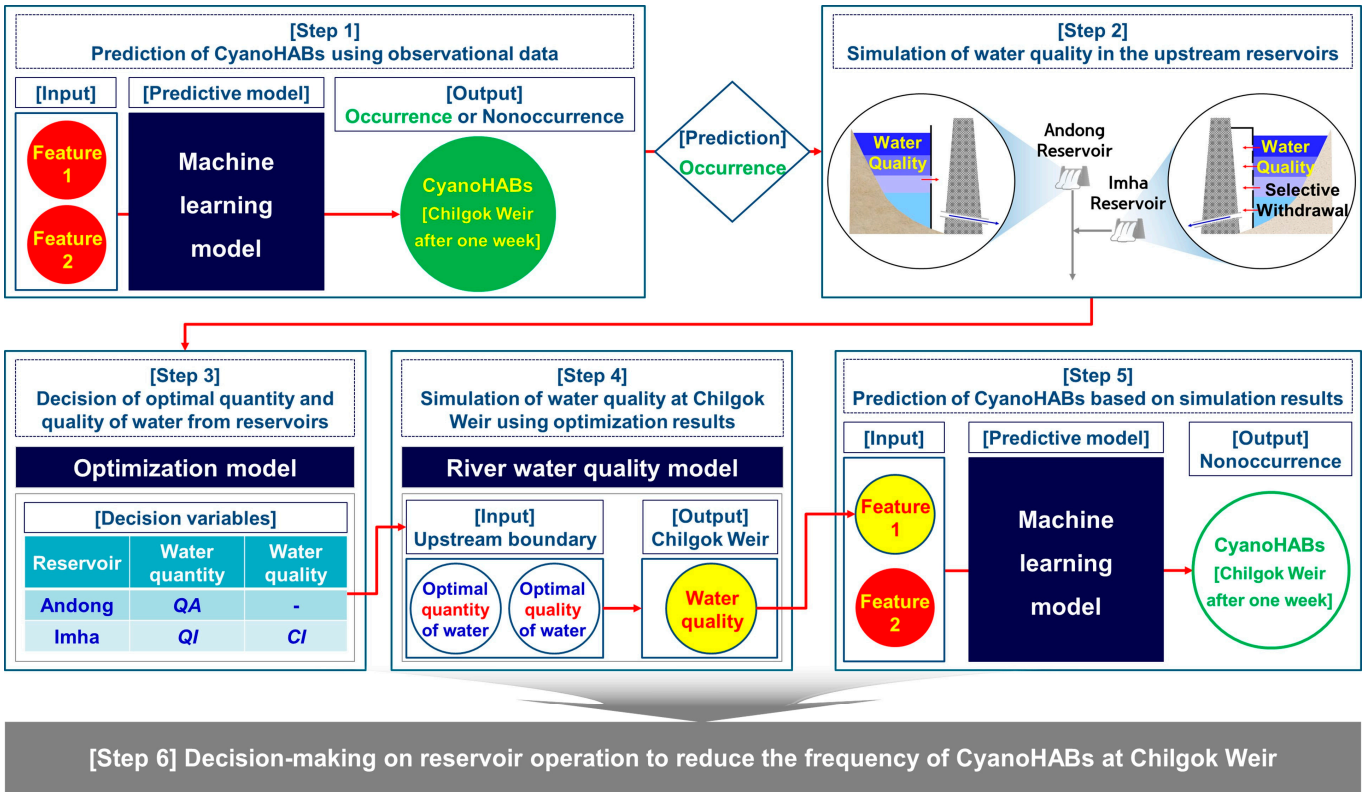


**Figure 2.** Decision support framework for optimal reservoir operation to reduce the frequency of CyanoHABs at Chilgok Weir.

This study focuses on presenting and applying a machine learning model in Steps 1 and 5, an optimization model in Step 3, and a river water quality model in Step 4. Although the simulation of the water quality of reservoirs in Step 2 is not included in this study, the applicability of this framework is demonstrated using observational data related to the quantity and quality of the Andong and Imha reservoirs.

### *2.3. Data Availability*

The modeling process for this study requires hydrological or hydraulic data, water quality data, and meteorological data. These data can be collected from the Water Resources Management Information System, the Water Environment Information System, and the Open Met Data Portal of South Korea [38]. Hydrological or hydraulic data and meteorological data are available on a daily basis, while water quality data are obtained on a weekly basis (48 or 36 times a year) for rivers and monthly basis for reservoirs at three depths [38].

All data should have the same time interval for the modeling process in this study. However, while hydraulic data and meteorological data are acquired at daily intervals, water quality data are obtained on a weekly or monthly basis. To address the problem of the mismatch between the time steps, we transformed the weekly or monthly water quality data into daily data using a step function. The step function involves using the same value as observational data of the previous time step until the data for the next time step are available [39,40], maintaining consistency between water quality measurements [41].

### *2.4. Modeling Methods*

#### 2.4.1. Machine Learning Model

The machine learning model for Steps 1 and 5 of the framework was developed through our previous study [42] to predict the occurrence of CyanoHABs one week ahead at Chilgok Weir. The determination of the occurrence of CyanoHABs was based on cyanobacterial cell density, as specified by the Algae Alert System of South Korea, with a threshold of 1000 cells $mL^{-1}$ [42,43]. If the cyanobacterial cell density was equal to or higher than this threshold, CyanoHABs were deemed to appear.

Warmer temperatures are generally favorable for CyanoHABs, as well as nutrient conditions, which was also confirmed in our model. After testing many potential influencing factors, including nutrients such as nitrogen and phosphorus, we selected nitrate nitrogen ($NO_3$-N) and average air temperature (AT) as the input features to build the machine learning model. The model, which was developed using these two input features and applying the k-NN algorithm, an instance-based learning classification technique, was found to ensure the best accuracy of 88% [42]. One of the input features, $NO_3$-N, showed a negative correlation with the occurrence of CyanoHABs after one week at Chilgok Weir, while the other input feature, AT, had a positive correlation [42].

#### 2.4.2. Optimization Model

We developed a multiobjective optimization model considering both the quantity and quality of water for Step 3 in the framework. The decision variables of the optimization included the amount of water supply downstream of the two reservoirs (Andong (*QA*) and Imha (*QI*)) and the quality of water (*CI*) released from the Imha Reservoir using the SWF. The water quality parameter used in this optimization process was $NO_3$-N, which was an input feature of the machine learning model presented in Section 2.4.1. Since the optimization problem involved the quantity and quality of water, we formulated two objective functions.

The first objective function (OF1) was related to water quantity, as shown in Equation (1). Through the joint operation of both reservoirs, the two reservoirs can be assumed as one in terms of water supply. In this regard, we aimed at minimizing OF1, which is the difference between the sum of water quantity released from the Andong (*QA*) and Imha (*QI*) reservoirs and the sum of the water demands (QWD) to be allocated by the two reservoirs.

$$\text{minOF1} = \left\{ \sum_{t=1}^{Days} \left[ \frac{\text{QWD}_t - (QA_t + QI_t)}{\text{QWD}_t} \right]^2 \right\} \div Days \quad (1)$$

where *Days* is the number of days for a simulation period.

The second objective function (OF2) to be minimized is related to water quality, as shown in Equation (2). It was formulated by subtracting the $NO_3$-N concentration (*CJ*) at the junction where the water from the two reservoirs meets from the reference concentration (CR). We formulated OF2 to maximize *CJ*, as $NO_3$-N concentration was negatively correlated with the occurrence of CyanoHABs after one week at Chilgok Weir (as stated in Section 2.4.1). However, this *CJ* was constrained in order not to exceed CR (Equation (3)). *CJ* was calculated using the quantity and quality of water from both reservoirs with the chemical mass balance equation (Equation (4)) [44,45].

$$\text{minOF2} = \left( \sum_{t=1}^{Days} \frac{\text{CR} - CJ_t}{\text{CR}} \right) \div Days \quad (2)$$

$$CJ \leq \text{CR} \quad (3)$$

$$Q_D C_D = Q_U C_U + \sum_{i=1}^{n} L_i \quad (4)$$

where $Q_D$ and $C_D$ represent the flow rate ($m^3\ s^{-1}$) and concentration ($mg\ L^{-1}$) of a specific water quality parameter at a downstream location, respectively. At an upstream location, these values are represented by $Q_U$ and $C_U$, respectively. $L_i$ ($g\ s^{-1}$) and n denote the individual loadings and the number of inflow points, respectively, between the upstream and downstream locations.

The quality of water (*CI*) released from the Imha Reservoir was constrained in consideration of the $NO_3$-N concentration distributed by the depth of the reservoir. The constraint on *CI* was set between the minimum (Min. CI) and maximum (Max. CI) values of the $NO_3$-N concentration, as shown in Equation (5), based on the depth where the SWF is available. The simulation of water quality is necessary to determine the distribution of $NO_3$-N concentration by the depth of a reservoir, as discussed in Step 2 of the framework. However, in this study, we demonstrated the applicability of the framework by using the observational data of the $NO_3$-N concentration by depth in the Imha Reservoir.

$$\text{Min. CI} \leq CI \leq \text{Max. CI} \quad (5)$$

Water quality in the Imha Reservoir is monitored at three stations: Imha Dam 1, Imha Dam 2, and Imha Dam 3. The daily data of Min. CI and Max. CI were retrieved from a total of four stations, including one station monitoring the quality of water downstream released from the Imha Reservoir. Figure 3 shows Min. CI and Max. CI.

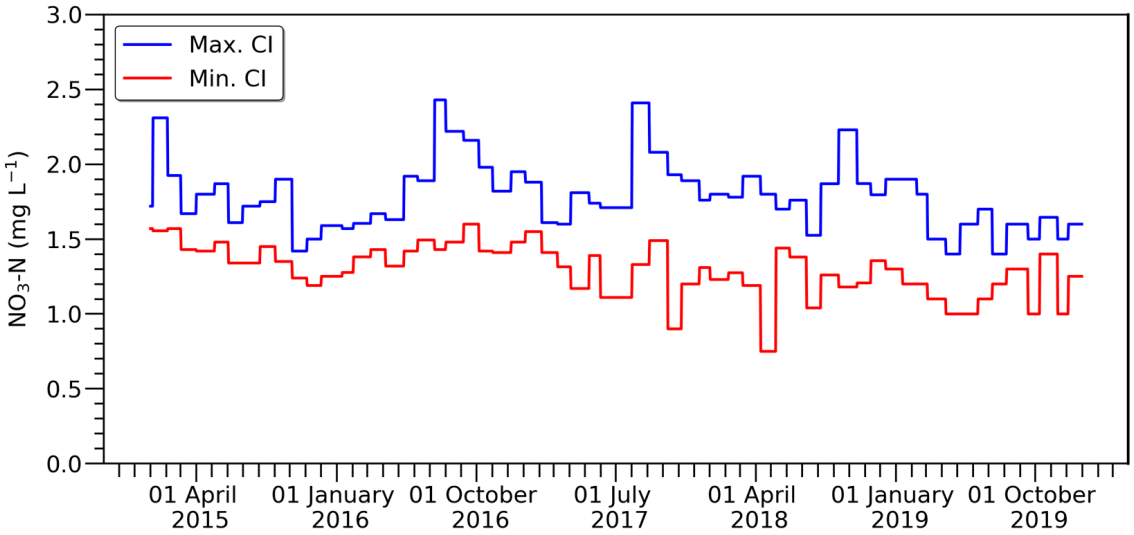


**Figure 3.** Range of $NO_3$-N concentrations (*CI*) in water released from the Imha Reservoir.

In the optimization model, we employed NSGA-II, a widely applied genetic algorithm using a fast nondominated sorting procedure [46]. The Python library pymoo (version 0.6.0) was used [47].

#### 2.4.3. River Water Quality Model

In our earlier study [48], we developed a river water quality model using HEC-RAS version 5.0.7 to simulate the $NO_3$-N dynamics at Chilgok Weir, given upstream boundary conditions. This model, evaluated to have a high performance of 0.76 or higher with both $R^2$ (Coefficient of Determination) and NSE (Nash Sutcliffe Efficiency) [48], was applied in Step 4 of the framework, since the model covered the same area as in this study.

The one-dimensional river water quality model using HEC-RAS, a process-based modeling system that can simulate the biogeochemical transformation processes of nitrogen

parameters [49], does not require long computation time. However, the HEC-RAS model first simulates unsteady flow and then water quality using the simulation results of the unsteady flow [49]. In order to apply the framework, repeatedly running the HEC-RAS model in the optimization process of Step 3 is necessary, which requires significant computational time.

To address this time-consuming computational issue, we developed a surrogate model that mimics the $NO_3$-N dynamics simulated by the HEC-RAS model, based on an artificial neural network (ANN). Such surrogate models, based on machine learning, when trained, are much more computationally efficient compared with process-based models [50]. The model was built based on Equation (6) [2–4] by using the hydraulic, water quality, and meteorological data obtained for developing the HEC-RAS model in our previous study [48]. The dataset for training and testing the surrogate model consisted of 508,923 instances, which were generated using the HEC-RAS model by varying the upstream boundary conditions, such as flow rate and $NO_3$-N concentration. This variation in the upstream boundary conditions was required to link the optimization results obtained from Step 3 with the surrogate model. The surrogate model *SM* was constructed using the Keras open-source software library in Python (version 3.8.10):

$$\hat{y}(t) = SM(x_1(t-1),\ x_1(t-2), \cdots,\ x_m(t-l)) \tag{6}$$

where $\hat{y}$ is the prediction result of the $NO_3$-N concentration at Chilgok Weir, *SM* is the surrogate model which emulates the behavior of the HEC-RAS model, $x$ ($x_1$, $x_2$,. . ., $x_m$) is a vector of input features, $t$ is the time step (day), $m$ is the number of input features, and $l$ is the time lag. Table 1 shows the list of the data used for the development of the surrogate model, which are the same data as for the HEC-RAS model.

**Table 1.** List of the data used for the development of the surrogate model.

| Category | Data | Unit |
|---|---|---|
| Hydraulic data | Flow rate | $m^3\ s^{-1}$ |
| | Water level | mamsl |
| Water quality data | Water temperature | °C |
| | Algae | $mg\ L^{-1}$ |
| | Dissolved oxygen (DO) | $mg\ L^{-1}$ |
| | Dissolved organic nitrogen (DON) | $mg\ L^{-1}$ |
| | Ammonium nitrogen ($NH_4$-N) | $mg\ L^{-1}$ |
| | Nitrite nitrogen ($NO_2$-N) | $mg\ L^{-1}$ |
| | Nitrate nitrogen ($NO_3$-N) | $mg\ L^{-1}$ |
| Meteorological data | Atmospheric pressure | hPa |
| | Air temperature | °C |
| | Relative humidity | % |
| | Solar radiation | $MJ\ m^{-2}$ |
| | Wind speed | $m\ s^{-1}$ |

While the surrogate model has the advantage to save computation time, it may not be able to reproduce all the HEC-RAS simulation results with 100% accuracy. Hence, we compared the simulation results of the surrogate model with those of the HEC-RAS model. To measure the performance of the surrogate model, indices such as $R^2$, NSE, and RMSE (Root Mean Square Error) were used. These performance indices are represented by Equations (7)–(9), respectively [51].

$$R^2 = \left[ \frac{\sum_{i=1}^{n} (O_i - \overline{O})(S_i - \overline{S})}{\sqrt{\sum_{i=1}^{n} (O_i - \overline{O})^2} \sqrt{\sum_{i=1}^{n} (S_i - \overline{S})^2}} \right]^2 \tag{7}$$

$$NSE = 1 - \frac{\sum_{i=1}^{n}(O_i - S_i)^2}{\sum_{i=1}^{n}(O_i - \overline{O})^2} \quad (8)$$

$$RMSE = \sqrt{\frac{1}{n}\sum_{i=1}^{n}(O_i - S_i)^2} \quad (9)$$

where $O$ is observational data and $S$ is simulation result.

### *2.5. Experimental Setup*

#### 2.5.1. Procedure

We established the procedure for demonstrating the applicability of the framework shown in Figure 2 in three stages: optimization, river water quality modeling, and simulation of the occurrence of CyanoHABs at Chilgok Weir. The first stage involves the optimization model, which simulates time series data for the decision variables *QA*, *QI*, and *CI*. These time series data are used for calculating the flow rate (*QJ*) and the $NO_3$-N concentration (*CJ*) at the junction where the water from the Andong and Imha Reservoirs converge. *QJ* can be different from *QA* + *QI*, since *QJ* includes the residual discharge for the area from the dam to the junction. In the second stage, the river water quality model runs the simulation of the $NO_3$-N dynamics at Chilgok Weir by using the calculated *QJ* and *CJ* as boundary conditions. Finally, the machine learning model is employed to predict the occurrence of CyanoHABs at Chilgok Weir. This model uses the $NO_3$-N concentration simulated in the second stage and the observational data of average air temperature as input features. Figure 4 shows the experimental procedure.

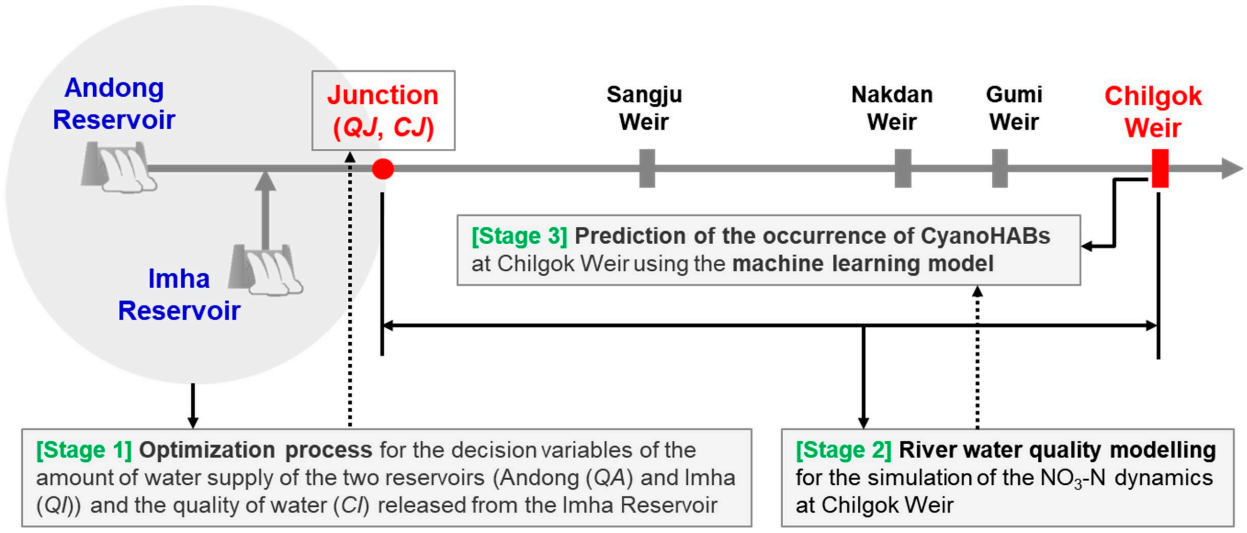


**Figure 4.** Experimental procedure.

We adopted the experimental procedure based on the observational data collected over five years from 2015 to 2019. During this period, there was no record of discharge via spillway for flood control from the Andong and Imha reservoirs, which was important, as this study did not consider flood routing in the reservoirs.

The observational data used in this study included the cyanobacterial cell density for 226 days, of which 72 days had a cell density of 1000 or higher. As mentioned in Section 2.4.1, we assumed that CyanoHABs occurred when the cell density was 1000 or higher. In this study, we compared the results of CyanoHABs simulated using the optimization results with the 72 days when they were observed.

Before following the experimental procedure, we took a simulation test to validate the developed models. As mentioned in Section 2.4.1, the $NO_3$-N concentration at Chilgok

Weir showed a negative correlation with the occurrence of CyanoHABs. In consideration of this relationship, two hypothetical scenarios were constructed by increasing or decreasing the $NO_3$-N concentration of the upstream boundary condition by 0.50 mg $L^{-1}$ from the values in the observational data. The river water quality model using HEC-RAS simulated the $NO_3$-N dynamics at Chilgok Weir under these scenarios. The machine learning model was used to simulate the number of days with CyanoHABs at Chilgok Weir, using the $NO_3$-N concentration simulated and the average air temperature measured.

#### 2.5.2. Experimental Cases for Optimization

We examined the effect of different constraints on the decision variables of the optimization process with nine cases, as shown in Table 2. These cases were based on five variables: *QA*, *QI*, *QA* + *QI*, *QJ*, and *CJ*.

**Table 2.** Experimental cases based on the constraints for the optimization process.

| Case | Constraints for Optimization | | | | |
|---|---|---|---|---|---|
| | ***QA*** **(Unit: $m^3$ $s^{-1}$)** | ***QI*** **(Unit: $m^3$ $s^{-1}$)** | ***QA* + *QI*** **(Unit: $m^3$ $s^{-1}$)** | ***QJ*** **(Unit: $m^3$ $s^{-1}$)** | ***CJ* (*CJ* ≤ CR)** **(Unit: mg $L^{-1}$)** |
| Case 1 | $0 \leq QA \leq 161.0$ | $1.0 \leq QI \leq 119.0$ | $QA + QI \leq$ QD | | $CJ \leq 3.11$ |
| Case 2 | | | | | $CJ \leq 3.50$ |
| Case 3 | $0 \leq QA \leq 0.5$QD | $1.0 \leq QI \leq 0.5$QD | - | $QJ \geq$ QWD | $CJ \leq 3.11$ |
| Case 4 | $0 \leq QA \leq 0.3$QD | $1.0 \leq QI \leq 0.7$QD | - | | $CJ \leq 3.11$ |
| Case 5 | $0 \leq QA \leq 0.7$QD | $1.0 \leq QI \leq 0.3$QD3 | - | | $CJ \leq 3.90$ |
| Case 6 | $0 \leq QA \leq 161.0$ | $0 \leq QI \leq 119.0$ | $QA+QI=$QO | | $CJ \leq 4.10$ |
| Case 7 | $0.500$QO $\leq QA \leq 0.505$QO | $0.500$QO $\leq QI \leq 0.505$QO | - | $QJ \geq 17.5$ | $CJ \leq 3.70$ |
| Case 8 | $0.300$QO $\leq QA \leq 0.305$QO | $0.700$QO $\leq QI \leq 0.705$QO | - | | $CJ \leq 3.50$ |
| Case 9 | $0.700$QO $\leq QA \leq 0.705$QO | $0.300$QO $\leq QI \leq 0.305$QO | - | | $CJ \leq 4.50$ |

QD, shown in Table 2, is the sum of the maximum amount of water supply allocated downstream in the design stage of the Andong and Imha Reservoirs, hereinafter referred to as "Design Discharge". This Design Discharge includes the water quantity for municipal and industrial use, irrigation, and environmental flow, and it is presented as monthly data, as shown in Table 3. The sum of the water demands downstream of the two reservoirs, referred to as QWD (as stated in Section 2.4.2), can also be presented as quantities by month, with slight variations from year to year. QO is the observational data for the water supply downstream of the two reservoirs. This QO was acquired on a daily basis, but it was converted into a monthly average for comparison with QD and QWD. The data for these variables (QD, QWD, and QO) are shown in Figure 5.

**Table 3.** Design Discharge.

| Reservoir | Design Discharge by Month (Unit: $m^3$ $s^{-1}$) | | | | | | | | | | | |
|---|---|---|---|---|---|---|---|---|---|---|---|---|
| | **Jan** | **Feb** | **Mar** | **Apr** | **May** | **Jun** | **Jul** | **Aug** | **Sep** | **Oct** | **Nov** | **Dec** |
| Andong | 19.9 | 19.9 | 19.9 | 20.8 | 33.7 | 49.3 | 40.5 | 50.2 | 36.4 | 22.0 | 19.9 | 19.9 |
| Imha | 13.5 | 13.5 | 13.5 | 13.6 | 14.0 | 14.7 | 14.4 | 14.8 | 14.2 | 13.6 | 13.5 | 13.5 |
| Sum (QD) | 33.4 | 33.4 | 33.4 | 34.4 | 47.7 | 64.0 | 54.9 | 65.0 | 50.6 | 35.6 | 33.4 | 33.4 |

The reference concentration of $NO_3$-N, denoted as CR, was used as a constraint on the $NO_3$-N concentration (*CJ*) at the junction of the water downstream from the two reservoirs (as mentioned in Section 2.4.2). In Case 1, Case 3, and Case 4, CR was set to 3.11 mg $L^{-1}$, the maximum concentration of $NO_3$-N at the junction retrieved from the observational data between 2015 and 2019. In Case 2, CR was set to 3.50 mg $L^{-1}$ in order to compare the results of Case 2 with those of Case 1. We made Case 2 to analyze the impact of variation in CR. For the remaining cases (Cases 5–9), CR was set to the minimum concentration of $NO_3$-N, at which the Pareto front could be obtained during the optimization process.

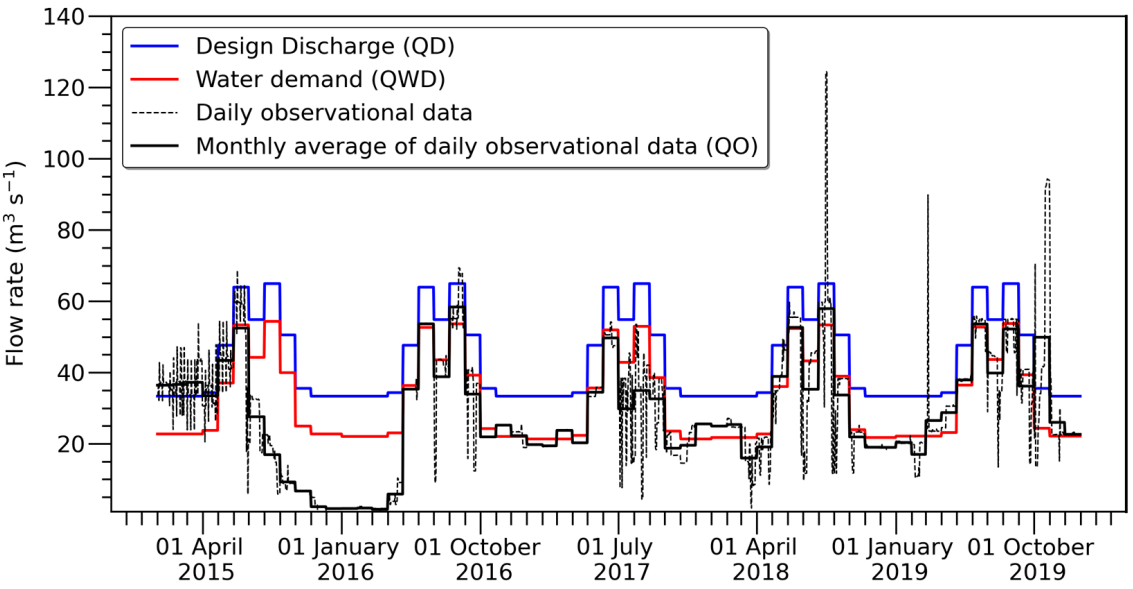


**Figure 5.** Graph showing Design Discharge, water demand, daily observational data, and monthly averages of the daily observational data for the downstream river (sum for the Andong and Imha Reservoirs).

In the first two cases, the maximum amounts of water were set to 161.0 $m^3$ $s^{-1}$ and 119.0 $m^3$ $s^{-1}$ for *QA* and *QI*, respectively. These values represent the quantities of water that can be released downstream through the hydropower generators of the two reservoirs. The minimum *QI* was set to 1.0 $m^3$ $s^{-1}$, which is a value that accounts for the water demand of a downstream river from the Imha Reservoir. This intake facility for the water demand is located between the Imha Dam and the junction where the Banbyeoncheon River, a downstream river of the Imha Reservoir, joins the Nakdong River.

We placed the constraints on the sum of water released from the two reservoirs (*QA* + *QI*) in Cases 1 and 2 to ensure that *QA* + *QI* did not exceed the Design Discharge (QD). Additionally, *QJ* was constrained to satisfy QWD, considering the joint operation of the two reservoirs. This constraint on *QJ* was also applied to Cases 3–5.

The major difference between Cases 3–5 and Cases 1–2 is in the constraints placed on *QA* and *QI*. In Cases 3–5, the maximum values of *QA* and *QI* were determined by applying to each portion of QD, where the sum of the portions equals one in each case. The goal of this approach was to reduce the number of constraints and narrow the range of constraints compared with Cases 1–2, allowing efficient optimization. To evaluate the impact of different portions on the simulation results for CyanoHABs, the values (in percentages) of 50%, 30%, and 70% were applied to Cases 3–5.

Unlike Cases 1–5, which were related to QD and QWD, Cases 6–9 were based on QO. Reservoirs are usually operated to meet water demand, but as shown in Figure 5, the amount of water released from the reservoir may be less than the water demand due to drought or the status of the flow rate downstream. To assess whether the frequency of occurrence of CyanoHABs downstream could be reduced by releasing a similar amount of water to the observed, the constraint on *QA* + *QI* in Case 6 was set to be equivalent to QO. In Cases 6–9, the constraint of *QJ* was set to exceed 17.5 $m^3$ $s^{-1}$, considering the stability of the water level calculation in the HEC-RAS model used after the optimization process. When values of water level for unsteady flow in each cross-section are calculated using HEC-RAS, a dry condition for a cross-section makes an error [49]. To avoid this error, a minimum flow rate is required, and the value of 17.5 $m^3$ $s^{-1}$ was used as the minimum flow rate for the HEC-RAS model in our previous study [48].

The difference between Case 6 and Cases 7–9 was in the constraints applied to *QA* and *QI*. In Cases 7–9, we applied the earlier defined portions to QO for the constraints on *QA* and *QI*, which narrowed the range of *QA* and *QI*, enabling efficient optimization.

We carried out the optimization for these nine cases and then simulated the number of days with CyanoHABs at Chilgok Weir using the river water quality model and the machine learning model. The simulation results allowed us to evaluate the impact of changing the optimization constraints on the number of days with CyanoHABs.

## 3. Results

### *3.1. Simulation Test*

We generated hypothetical data by modifying the observational data of the $NO_3$-N concentrations by increments or decrements of 0.50 mg $L^{-1}$ for the simulation test, as stated in Section 2.5.1. These data were used as the upstream boundary condition for the HEC-RAS model. The other boundary conditions and model data remained unchanged. Figure 6 shows the results of the simulation test in terms of $NO_3$-N concentration at Chilgok Weir. Table 4 shows the number of days with CyanoHABs after one week at Chilgok Weir, obtained after applying the machine learning model based on the $NO_3$-N concentration shown in Figure 6.

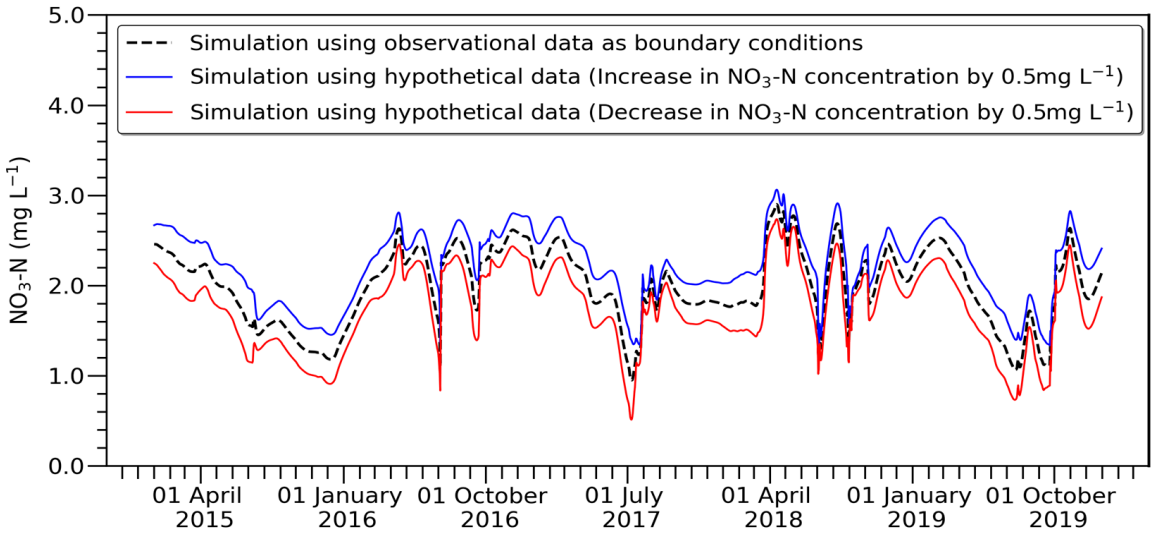


**Figure 6.** Results of the simulation test (the $NO_3$-N concentrations at Chilgok Weir using the hypothetical data and the HEC-RAS model).

**Table 4.** Results of the simulation test (the number of days with CyanoHABs after one week at Chilgok Weir using the $NO_3$-N concentrations of Figure 6).

| CyanoHABs | Observation | Increment of 0.50 mg $L^{-1}$ | Decrement of 0.50 mg $L^{-1}$ |
|---|---|---|---|
| Occurrence | 72 days | 66 days | 103 days |
| Nonoccurrence | 154 days | 160 days | 123 days |
| Sum | 226 days | 226 days | 226 days |

The results of the simulation test showed a negative correlation between the $NO_3$-N concentration upstream and the number of days with CyanoHABs, as shown in Table 4. These findings indicated that an increase in the $NO_3$-N concentration upstream resulted in a decrease in the number of days with CyanoHABs at Chilgok Weir, as expected. Hence, the simulation results demonstrate the validity of both the machine learning model and the HEC-RAS model.

### *3.2. Optimization for the Quantity and Quality of Water Released from the Reservoirs*

We simulated the time series data for the decision variables, *QA*, *QI*, and *CI*, corresponding to a period of 1826 days over five years from 2015 to 2019 by applying the two objective functions presented in Section 2.4.2. The optimization process involved the application of constraints for the nine cases outlined in Section 2.5.2. The optimization results were obtained as shown in Figure A1 of Appendix B, which presents the Pareto front for each case.

The differences were minor between the optimal solutions, as shown through the range of the OF1 axis and OF2 axis in Figure A1. This would lead to only small variations between the decision variables for the solutions. To further examine the relationship between the decision variables and the optimal solutions, three optimal solutions were selected for each case, as shown in Figure A1. These included a solution of most minimizing the first objective function (OF1 min.), a solution of most minimizing the second objective function (OF2 min.), and a median of the optimal solutions. The simulation results, as shown in Figure A2 of Appendix B, confirmed slight differences between the decision variables (*QA* + *QI* and *CI*) corresponding to the three selected solutions in the nine cases.

Figure A3 of Appendix B shows the results of *QJ* and *CJ* simulated by the constraints specified in the nine cases. These *QJ* and *CJ* were used as the upstream boundary conditions for the river water quality model. In Cases 1–5, the simulation results indicate that the values of *QJ* were consistently greater than or equal to QWD throughout the entire period. On the other hand, the simulation results of Cases 6–9 showed that the values of *QJ* might be lower than QWD. This is because Cases 6–9 used the observation data (QO) as the constraint on *QA* + *QI*, as shown in Table 2. Furthermore, the simulation results confirm that *CJ* did not exceed the CR specified in each case.

### *3.3. $NO_3$-N Dynamics at Chilgok Weir*

The $NO_3$-N dynamics at Chilgok Weir were simulated by using the *QJ* and *CJ* values for the three optimal solutions (OF1 min., OF2 min., and median) as the upstream boundary conditions for the river water quality model. We used two models for the simulation: the HEC-RAS model and the surrogate model. The surrogate model was developed to replicate the $NO_3$-N dynamics simulated by the HEC-RAS model, as mentioned in Section 2.4.3.

We assessed the performance of the surrogate model by using both the graphical method and the traditional performance indices, such as $R^2$, NSE, and RMSE. Figure 7 shows the simulation results of the $NO_3$-N concentrations at Chilgok Weir for Case 1. Although the simulation results of the two models were not 100% identical, the trend of the $NO_3$-N concentration, whether increasing or decreasing, was almost the same. The performance indices for the surrogate model are shown in Table 5. $R^2$ and NSE were higher than 0.90 and 0.80, respectively. In addition, RMSE was less than 0.20 for all cases. Based on these performance measures, the performance of the surrogate model can be judged as high. Furthermore, the surrogate model had the advantage of saving computation time by approximately 1/3 or 1/4 compared with the HEC-RAS model.

**Table 5.** Performance of the surrogate model for three optimal solutions.

| Case | $R^2$ | | | NSE | | | RMSE | | |
|---|---|---|---|---|---|---|---|---|---|
| | OF1 min. | OF2 min. | Median | OF1 min. | OF2 min. | Median | OF1 min. | OF2 min. | Median |
| Case 1 | 0.921 | 0.921 | 0.920 | 0.910 | 0.912 | 0.911 | 0.129 | 0.129 | 0.129 |
| Case 2 | 0.918 | 0.917 | 0.918 | 0.908 | 0.908 | 0.908 | 0.131 | 0.132 | 0.131 |
| Case 3 | 0.915 | 0.912 | 0.914 | 0.887 | 0.880 | 0.884 | 0.136 | 0.138 | 0.137 |
| Case 4 | 0.905 | 0.902 | 0.905 | 0.846 | 0.837 | 0.842 | 0.154 | 0.155 | 0.155 |
| Case 5 | 0.907 | 0.906 | 0.907 | 0.896 | 0.893 | 0.895 | 0.138 | 0.139 | 0.138 |
| Case 6 | 0.954 | 0.954 | 0.954 | 0.948 | 0.947 | 0.947 | 0.098 | 0.098 | 0.098 |
| Case 7 | 0.943 | 0.943 | 0.943 | 0.920 | 0.919 | 0.919 | 0.118 | 0.119 | 0.119 |
| Case 8 | 0.932 | 0.932 | 0.932 | 0.884 | 0.881 | 0.882 | 0.140 | 0.142 | 0.141 |
| Case 9 | 0.943 | 0.943 | 0.943 | 0.935 | 0.934 | 0.934 | 0.110 | 0.110 | 0.110 |

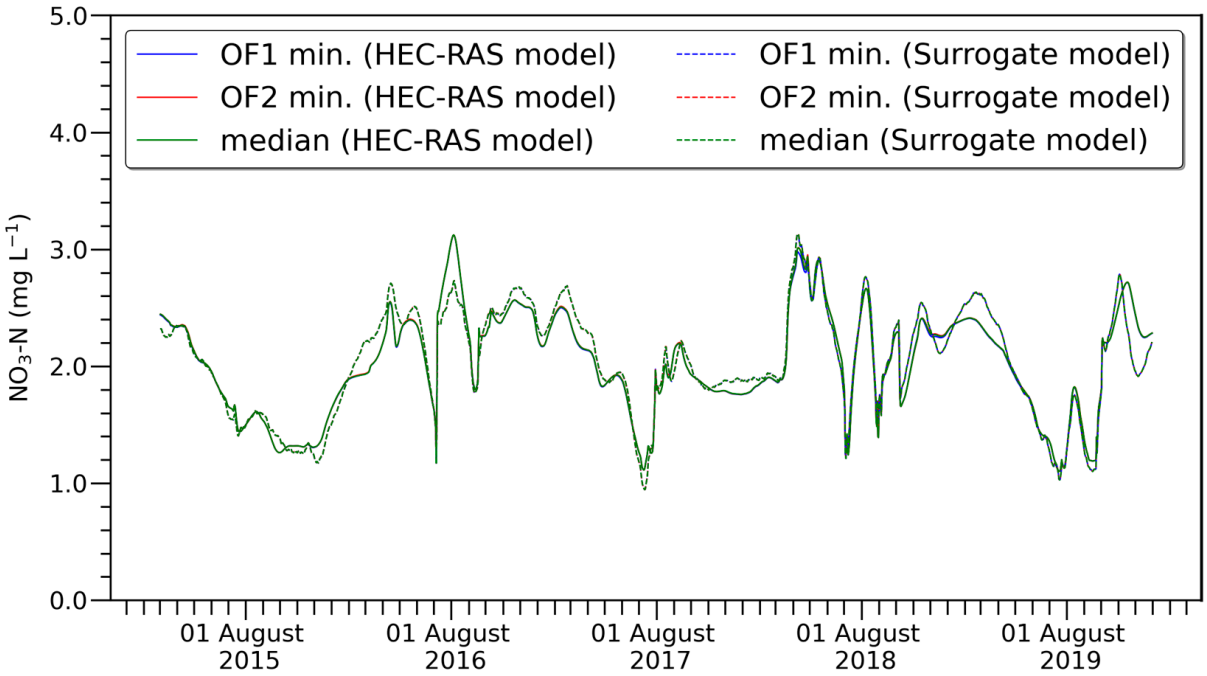


**Figure 7.** Simulation results of the $NO_3$-N concentrations at Chilgok Weir using the HEC-RAS model and the surrogate model for three optimal solutions.

### *3.4. Prediction of the Occurrence of CyanoHABs at Chilgok Weir*

We simulated the number of days with CyanoHABs after one week at Chilgok Weir for three optimal solutions, as shown in Table 6. The simulation results were obtained by using the $NO_3$-N concentrations simulated by the river water quality model. Given the importance of ensuring the accuracy of the river water quality model in this study, we analyzed the simulation results based on the HEC-RAS model.

**Table 6.** Simulation results of the number of days with CyanoHABs after one week at Chilgok Weir for three optimal solutions.

| Case | The Number of Days with CyanoHABs (Unit: Days) | | |
|---|---|---|---|
| | OF1 Min. | OF2 Min. | Median |
| Case 1 | 71 | 72 | 70 |
| Case 2 | 68 | 69 | 69 |
| Case 3 | 67 | 70 | 68 |
| Case 4 | 62 | 61 | 62 |
| Case 5 | 71 | 73 | 72 |
| Case 6 | 75 | 74 | 75 |
| Case 7 | 69 | 69 | 69 |
| Case 8 | 70 | 73 | 72 |
| Case 9 | 70 | 70 | 70 |

By comparing the observational data of 72 days with a cyanobacterial cell density of 1000 or higher from 2015 to 2019, we assessed the effect of reducing the number of days with CyanoHABs for nine cases. The results show that except for Case 6, the number of days was 72 or less in eight cases. Therefore, the applicability of the framework for the optimal operation of reservoirs was demonstrated in terms of reducing the frequency of CyanoHABs at Chilgok Weir.

Case 4 had the most noticeable effect in reducing the number of days with CyanoHABs among the nine cases. This simulation result of Case 4 would appear to be related to the constraint on the maximum amount of water from the Imha Reservoir, which accounted

for 70% of the Design Discharge (QD). This is because increasing the amount of water from the Imha Reservoir would raise the likelihood of increasing the pollution load of $NO_3$-N downstream, as water quality could be regulated from the reservoir using the SWF. On the other hand, Case 6 showed the simulation result exceeding 72 days, despite the fact that Case 6 had the objective functions and constraints which were formulated for the same purpose of reducing the number of days with CyanoHABs as the other cases.

As shown in Figure A2k,l for Case 6, *CI* for the optimal solutions varied near Min. CI while *QA* + *QI* was constrained on QO. This means that the variation in *CI* more greatly affected not only *CJ* but also the $NO_3$-N concentrations at Chilgok Weir than *QA* + *QI*. Comparing Case 6 with Cases 7–9, the values of *CI* for Cases 7–9 varied near Max. CI, as shown in Figure A2m–r, even if the simulation results of water quantity for Cases 7–9 were similar to those for Case 6. As a result, the number of days with CyanoHABs at Chilgok Weir increased since *CI* ($NO_3$-N concentration) for Case 6 was low.

Interestingly, the simulation results in Cases 1 and 2 reveal that the effect of reducing the number of days with CyanoHABs would be produced with only the constraint on the water quality. The performance of Case 2 outweighed that of Case 1. In Cases 1 and 2, the reference concentrations (CR) were 3.11 mg $L^{-1}$ and 3.50 mg $L^{-1}$, respectively. The other constraints in the two cases were the same. This result shows insight into how to reduce the frequency of occurrence of CyanoHABs downstream by controlling the quality of water from a reservoir by using an SWF, even with the same amount of water.

Among the simulation results in Cases 7–9, the reducing effect of the number of days with CyanoHABs was most significant in Case 7, followed by Case 9 and then Case 8. Cases 7–9 imposed constraints on the quantity of water based on the observational data (QO). These simulation results indicate that the optimal joint operation of the two reservoirs would lead to a reduction in the number of days with CyanoHABs using the same amount of water from the two reservoirs as the observational data. Nonetheless, the effect of Case 7 (69 days) was not as remarkable as that of Case 4 (61–62 days), where the constraint on the water quantity was set based on the water demand (QWD) and QD. These simulation results suggest that the quantity of water from the reservoirs can have an impact on the $NO_3$-N loadings downstream.

The simulation results for the given cases confirmed that optimal operation of reservoirs, which simultaneously consider both the quantity and quality of water, would effectively decrease the frequency of CyanoHABs downstream. However, this method may not always be practical, as in Case 6, where the simulation result showed the number of days exceeding 72. This outcome was likely due to the indirect use of optimization results (*QJ* and *CJ*), which served as upstream boundary conditions of the river water quality model, for predicting the occurrence of CyanoHABs at Chilgok Weir. Thus, to achieve tangible results in reducing the frequency of CyanoHABs downstream, the series of processes outlined in the framework should take place in an orderly and systemic manner.

## 4. Discussion

### *4.1. Insights Gained from this Case Study*

#### 4.1.1. Theoretical Aspects of CyanoHABs

This research focused on controlling the $NO_3$-N concentration in the river to reduce the frequency of occurrence of CyanoHABs, since $NO_3$-N was selected as an input feature of the machine learning model. Choosing $NO_3$-N as an input feature was the result of the feature selection based on not only the theoretical knowledge of CyanoHABs but also a rational approach to data analysis [42].

Nonetheless, this study may have limitations regarding the ecological parameters considered, because factors such as TN (Total Nitrogen) and TP that are widely recognized as main predictors for CyanoHABs [19] were not incorporated in the input features of the machine learning model. Further research can be conducted by using models with multiple combinations of input features, combined with Interpretable Artificial Intelligence (IAI) and eXplainable Artificial Intelligence (XAI) that provide post hoc explanations based

on ecological aspects [52]. Additionally, in the process of selecting input features (water quality data) related to the occurrence of CyanoHABs, a more theoretical understanding of the complex mechanisms of algal growth can be necessary, and detailed consideration related to the generation process of water quality data may be required.

CyanoHABs are widely known to frequently occur in a condition of nutrient overenrichment, such as nitrogen and phosphorous [53–55]. Nevertheless, $NO_3$-N was negatively correlated with the occurrence of CyanoHABs at Chilgok Weir, as shown in our previous study [42] stated in Section 2.4.1. Interestingly, while a positive correlation between nitrogen compounds and CyanoHABs is widely accepted, there is considerable variability depending on site-specific factors and cyanobacteria species present [7,19,56–59]. This highlights the need for context-specific approaches to managing freshwater systems, which take into account local conditions and the ecology of the system.

Despite the importance of identifying cyanobacteria species, the dataset on cyanobacterial cell density was not split into the groups of harmful cyanobacteria genera when developing the machine learning model. This was because analysis considering cyanobacteria species could cause the problem of an insufficient number of instances for the dataset. Hence, this machine learning model has limitations, since it did not involve the distinction of different cyanobacteria species.

In addition, because of this relationship between $NO_3$-N and CyanoHABs at Chilgok Weir, releasing water with a high concentration of $NO_3$-N from the reservoirs can decrease the frequency of CyanoHABs. However, this reservoir operation may cause the problem of increasing the $NO_3$-N concentration in a downstream river. Therefore, constraints on $NO_3$-N for the optimization process should be carefully formulated to address this issue. In this regard, we imposed constraints on the $NO_3$-N concentration downstream using the reference concentration (CR). These constraints enabled the $NO_3$-N concentration downstream to be maintained below CR. Accordingly, by considering an acceptable standard in the $NO_3$-N concentration for drinking water in the optimization process, a risk from contaminated water by an increased concentration of $NO_3$-N can be avoided.

#### 4.1.2. Practical Aspects of the Framework

The framework established in this study offers a methodology not to prevent the occurrence of CyanoHABs but to reduce their frequency. Nevertheless, the framework has advantages in terms of efficiency for two reasons. First, it can decrease the frequency of CyanoHABs in rivers without incurring any costs, unlike the current technologies for algae removal [60]. Second, the optimal operation of reservoirs does not require an additional amount of water, unlike the reservoir operation which has been involved in flushing water to reduce the frequency of CyanoHABs in a river downstream. Therefore, this framework related to the management of water quality can efficiently support sustainable development in terms of human health and the management of aquatic ecosystems [61,62].

However, this study also has limitations. First, this study did not consider flood routing in the reservoirs. In this regard, we used observational data from 2015 to 2019 that did not have a record of discharge through the spillway for flood control of the Andong and Imha Reservoirs. Secondly, errors in the river water quality model, particularly in the surrogate model, had an apparently negative impact on the simulation results of the occurrence of CyanoHABs. Thirdly, this research was conducted using observational data on water quality, but information related to land-use patterns that can affect water quality was not considered. Further studies are needed to transcend these limitations by dealing with the optimization process considering the simulation of flood routing in reservoirs, the performance improvement of river water quality models, and consideration of land use patterns of the study area.

This study did not incorporate the simulation of water quality in reservoirs corresponding to Step 2 of the framework. This decision was made based on the objective of this study, which was aimed at demonstrating the applicability of the framework using observational data on water quality in the two reservoirs. The practical application of the

framework can be possible through the use of modeling systems, such as CE-QUAL-W2, EELCOM-CAEDYM, and EFDC, for the simulation of water quality in reservoirs [63].

### *4.2. Challenges Related to Data Collection*

One of the most significant factors in developing a robust predictive model is data availability [64,65]. Fortunately, data on CyanoHABs, including cyanobacterial cell density, have been regularly examined and managed by the environmental authority in South Korea. However, obtaining water quality data is more difficult than collecting data on water quantity. This is because most water quality data are generally collected in situ and obtained in laboratory experiments. In this regard, these water quality data are available on a weekly or monthly basis.

Water quality modeling requires hydrological or hydraulic data and meteorological data collected at least on a daily basis as well as water quality data. The problem of differences in the time interval between these data may affect the performance of the predictive model. To resolve this problem, the need for frequently collecting water quality has arisen. Emerging technologies such as real-time and on-site data collection based on remote sensing and the Internet of Things [65,66] can be pragmatic solutions to the problem.

### *4.3. Further Improvements in Models and Decision Support Tools*

This study can offer scalability for enhancing sustainable development when linked to ecological assessments in a river. The impact of mitigating CyanoHABs on the aquatic ecosystem can first be analyzed, and the analysis result can be included as a factor of reservoir operation [62]. Further studies on the reservoir operation considering ecological assessments will be able to suggest innovative approaches in terms of the diversity of aquatic ecology in addition to the quantity and quality of water.

As the framework established in this study focused on only one specific location, the Chilgok Weir, further studies can be aimed at reducing the incidence of CyanoHABs at multiple locations. If the main predictors for CyanoHABs depend on a location, machine models, river water quality models, and optimization models should be developed corresponding to each location. Machine learning models first need to be developed corresponding to multiple locations, and the main predictors of the occurrence of CyanoHABs should be selected for each location. River water quality models can be built for each location to simulate the dynamics of the multiple parameters of water quality selected as the main predictors. An optimization model can be designed to address objective functions regarding water quantity and the multiple parameters of water quality. To simplify the objective functions, a water quality index can incorporate the multiple parameters of water quality [3].

## 5. Conclusions

In this study, we presented a framework for a decision support system aimed at reducing the frequency of CyanoHABs at Chilgok Weir of the Nakdong River in South Korea based on the multiobjective optimization of the joint operation of the Andong and Imha Reservoirs. The simulation results using observational data from 2015 to 2019 show that the implementation of this framework would reduce the number of days with CyanoHABs downstream by up to 15%. Accordingly, this new approach to reservoir operation considering both the quantity and quality of water had applicability to mitigating CyanoHABs downstream. Additionally, the framework is a novelty in terms of resource use and resource efficiency, as it can be a part of a solution to the problem of CyanoHABs without using an additional amount of water from a reservoir. Furthermore, this framework will work more effectively when simultaneously applying the technologies for physical, biological, or chemical algae removal technologies [67].

This research can make a contribution towards expanding the scope of the role of reservoirs from only ensuring water supply to improving the water environment of rivers. Furthermore, the research context would lead to a paradigm shift in reservoir operation, as there is increasing demand for clean water. However, for the paradigm shift in reservoir operation, reservoirs should be equipped with SWFs, or the joint operation of reservoirs must be carried out as shown in this study. Agencies in charge of reservoir operation need to recognize the necessity for these structural or nonstructural measures. This is because these measures will be one of the solutions to problems with water quality caused by climate change and thus will support sustainable development in the water sector.

**Author Contributions:** Conceptualization, D.P.S., A.J. and J.K.; methodology, D.P.S., A.J. and J.K.; software, J.K.; validation, J.K.; formal analysis, J.K.; investigation, J.K.; data curation, J.K.; writing—original draft preparation, J.K.; writing—review and editing, D.P.S., P.L.M.G. and A.J.; visualization, J.K.; supervision, D.P.S., P.L.M.G. and A.J. All authors have read and agreed to the published version of the manuscript.

**Funding:** This research received no external funding. The APC was funded by Delft University of Technology.

**Institutional Review Board Statement:** Not applicable.

**Informed Consent Statement:** Not applicable.

**Data Availability Statement:** The raw data are publicly available at http://www.wamis.go.kr for hydrological and hydraulic data (accessed on 14 March 2022), https://water.nier.go.kr for water quality data (accessed on 28 December 2022), and https://data.kma.go.kr for meteorological data (accessed on 18 April 2022).

**Acknowledgments:** We thank K-water (Korea Water Resources Corporation) for financially supporting the first author.

**Conflicts of Interest:** The authors declare no conflict of interest.

## Appendix A

Abbreviations used in this study are shown in Table A1.

**Table A1.** List of abbreviations (alphabetical order).

| Abbreviation | Description |
|---|---|
| ANN | Artificial Neural Network |
| AT | Average air Temperature |
| BOD | Biochemical Oxygen Demand |
| $C_D$ | Concentration of a specific water quality parameter at a Downstream location |
| $CI$ | Quality of water released from the Imha Reservoir |
| $CJ$ | $NO_3$-N concentration at the Junction where the water from the two reservoirs (Andong and Imha) meets |
| CR | Reference Concentration |
| $C_U$ | Concentration of a specific water quality parameter at an Upstream location |
| CyanoHABs | Harmful Cyanobacterial Blooms |
| DO | Dissolved Oxygen |
| DON | Dissolved Organic Nitrogen |
| k-NN | k-Nearest Neighbor |
| $L_i$ | Individual Loadings of Inflow points between upstream and downstream locations |
| Min. | Minimum |
| Max. | Maximum |
| $NH_4$-N | Ammonium Nitrogen |

**Table A1.** *Cont.*

| Abbreviation | Description |
|---|---|
| $NO_2$-N | Nitrite Nitrogen |
| $NO_3$-N | Nitrate Nitrogen |
| NSE | Nash Sutcliffe Efficiency |
| NSGA-II | Nondominated Sorting Genetic Algorithm II |
| OF1 | Objective Function 1 |
| OF2 | Objective Function 2 |
| $PO_4$ | Phosphate |
| *QA* | Amount of water supply downstream of the Andong Reservoir |
| $Q_D$ | Flow rate at a Downstream location |
| QD | Design Discharge |
| *QI* | Amount of water supply downstream of the Imha Reservoir |
| *QJ* | Flow rate at the Junction where the water from the two reservoirs (Andong and Imha) meets |
| QO | Observational data for the water supply downstream of the two reservoirs (Andong and Imha) |
| $Q_U$ | Flow rate at an Upstream location |
| QWD | Sum of the Water Demand allocated to the two reservoirs (Andong and Imha) |
| $R^2$ | Coefficient of Determination |
| RMSE | Root Mean Square Error |
| *SM* | Surrogate Model |
| SWF | Selective Withdrawal Facility |
| TP | Total Phosphorus |

## Appendix B

The optimization results in Section 3.2 are shown in Figures A1–A3.

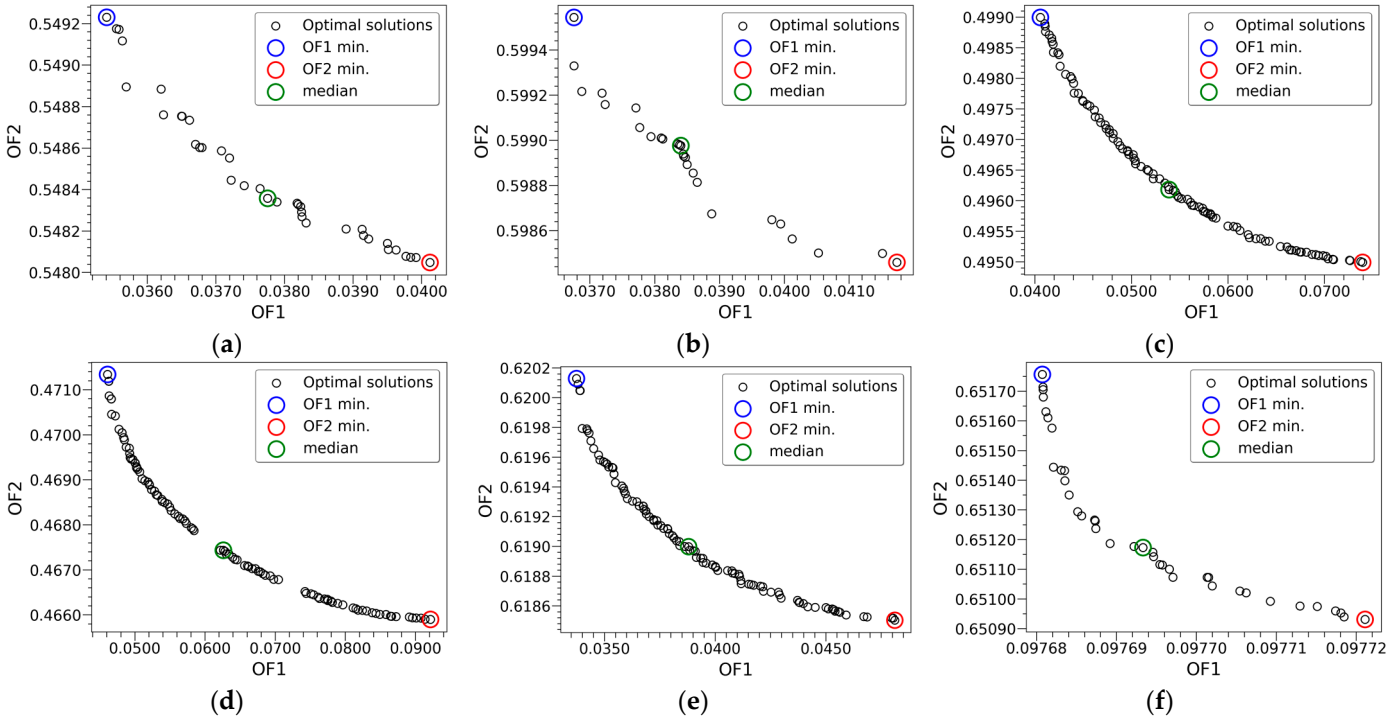


**Figure A1.** *Cont.*

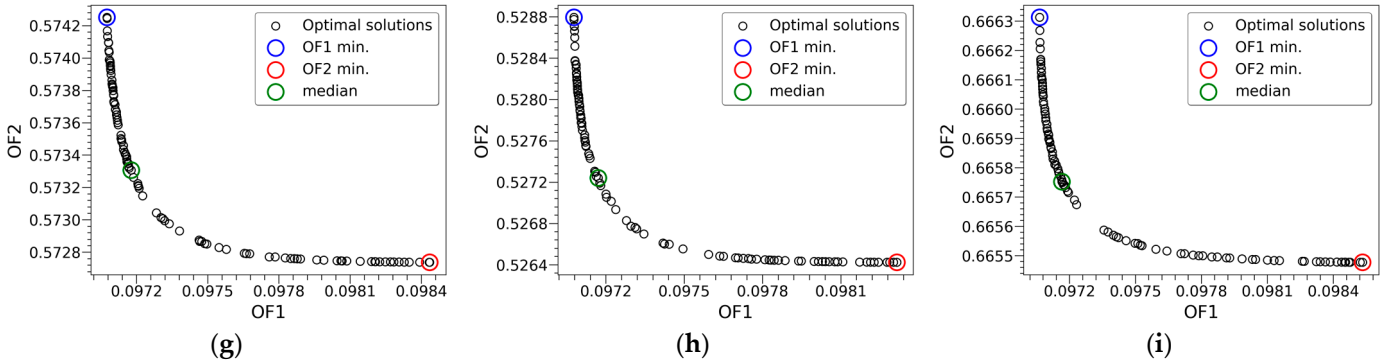


**Figure A1.** Pareto front (OF1 and OF2 are the objective functions related to water quantity and water quality, respectively): (**a**) Case 1; (**b**) Case 2; (**c**) Case 3; (**d**) Case 4; (**e**) Case 5; (**f**) Case 6; (**g**) Case 7; (**h**) Case 8; (**i**) Case 9.

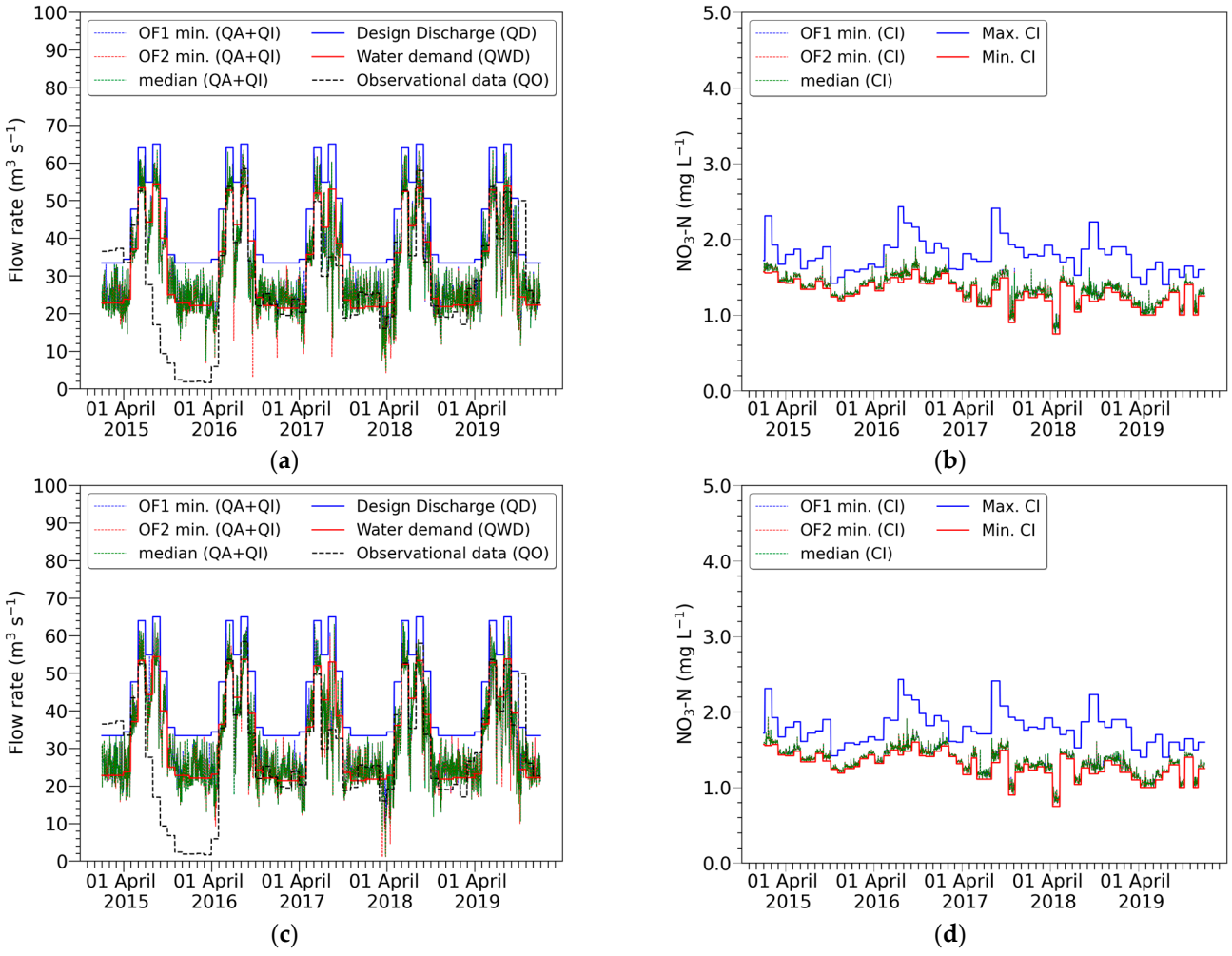


**Figure A2.** *Cont.*

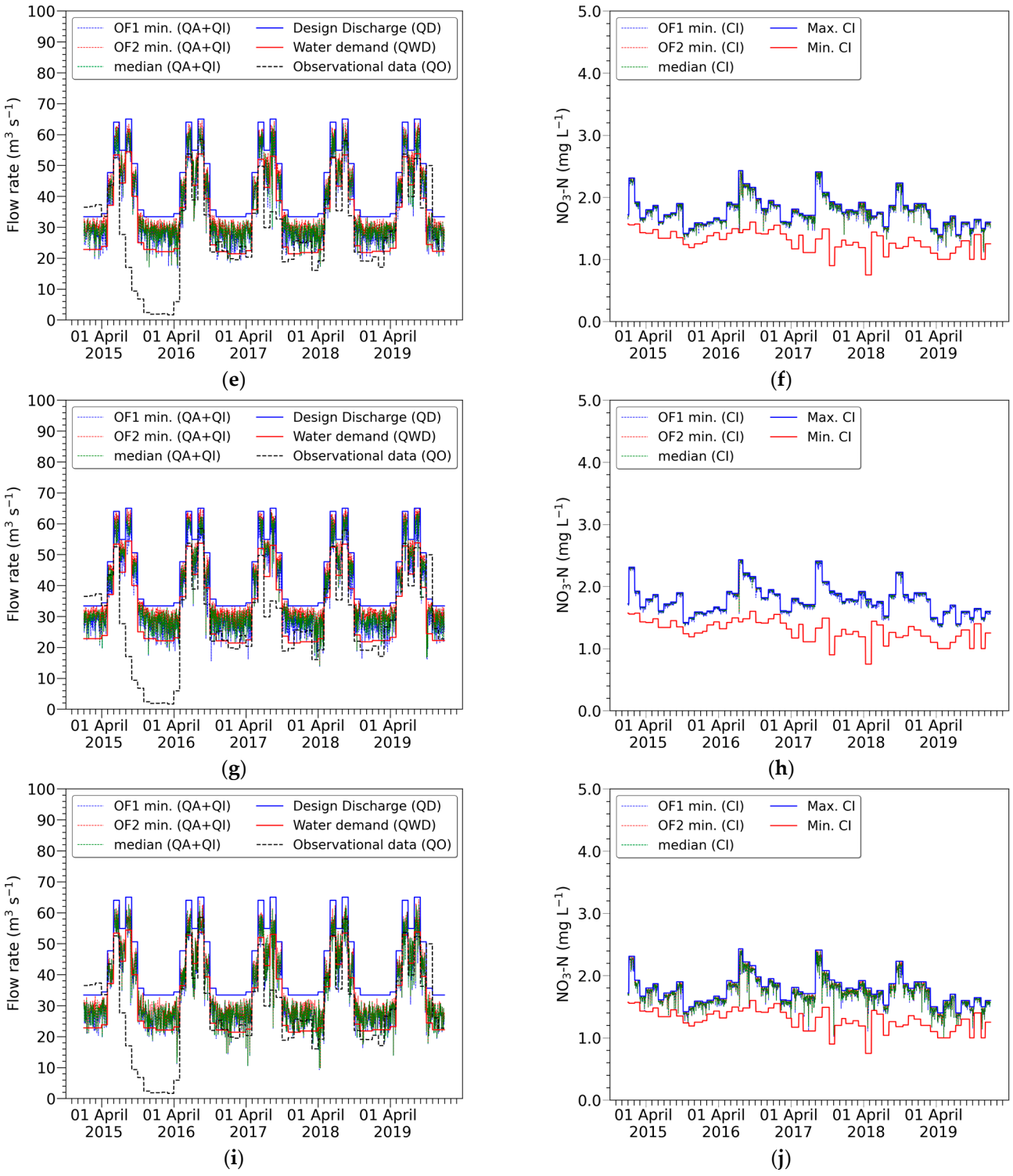


**Figure A2.** *Cont.*

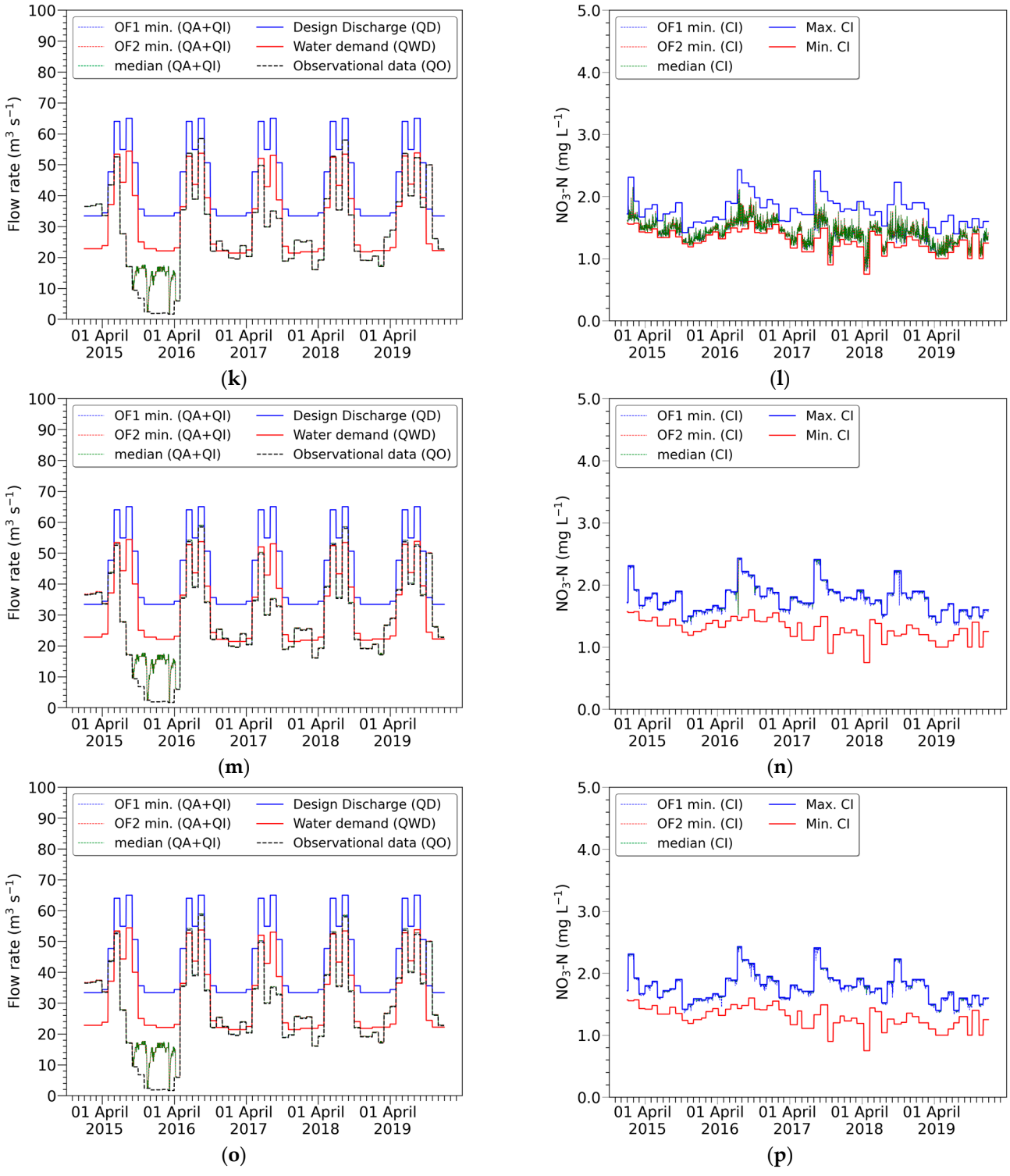


**Figure A2.** *Cont.*

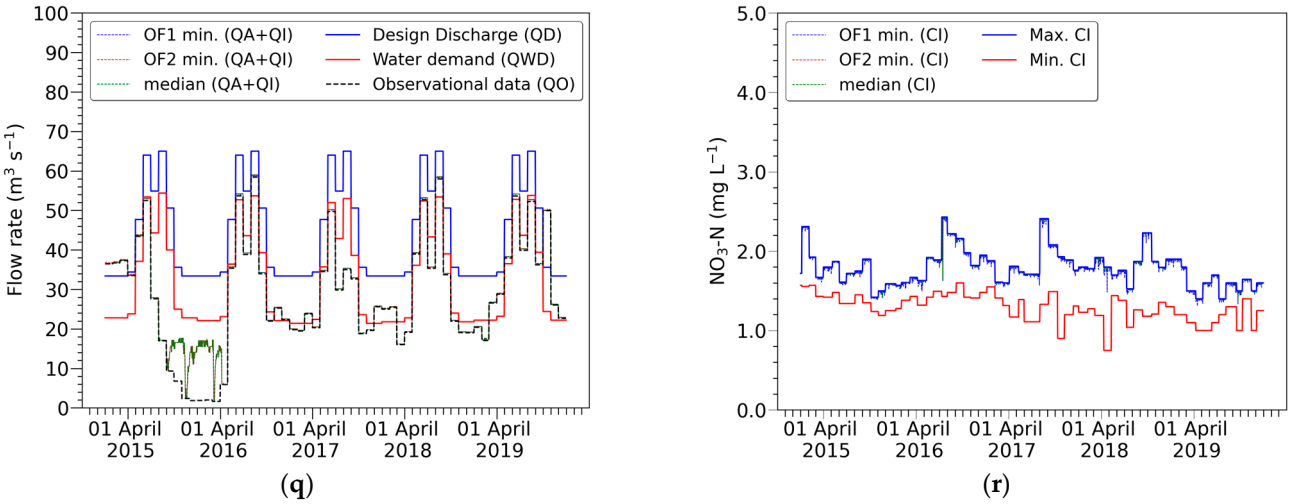


**Figure A2.** Optimization results (*QA* + *QI* and *CI*) for three optimal solutions (OF1 min., OF2 min., and median): (**a**) *QA* + *QI* for Case 1; (**b**) *CI* for Case 1; (**c**) *QA* + *QI* for Case 2; (**d**) *CI* for Case 2; (**e**) *QA* + *QI* for Case 3; (**f**) *CI* for Case 3; (**g**) *QA* + *QI* for Case 4; (**h**) *CI* for Case 4; (**i**) *QA* + *QI* for Case 5; (**j**) *CI* for Case 5; (**k**) *QA* + *QI* for Case 6; (**l**) *CI* for Case 6; (**m**) *QA* + *QI* for Case 7; (**n**) *CI* for Case 7; (**o**) *QA* + *QI* for Case 8; (**p**) *CI* for Case 8; (**q**) *QA* + *QI* for Case 9; (**r**) *CI* for Case 9.

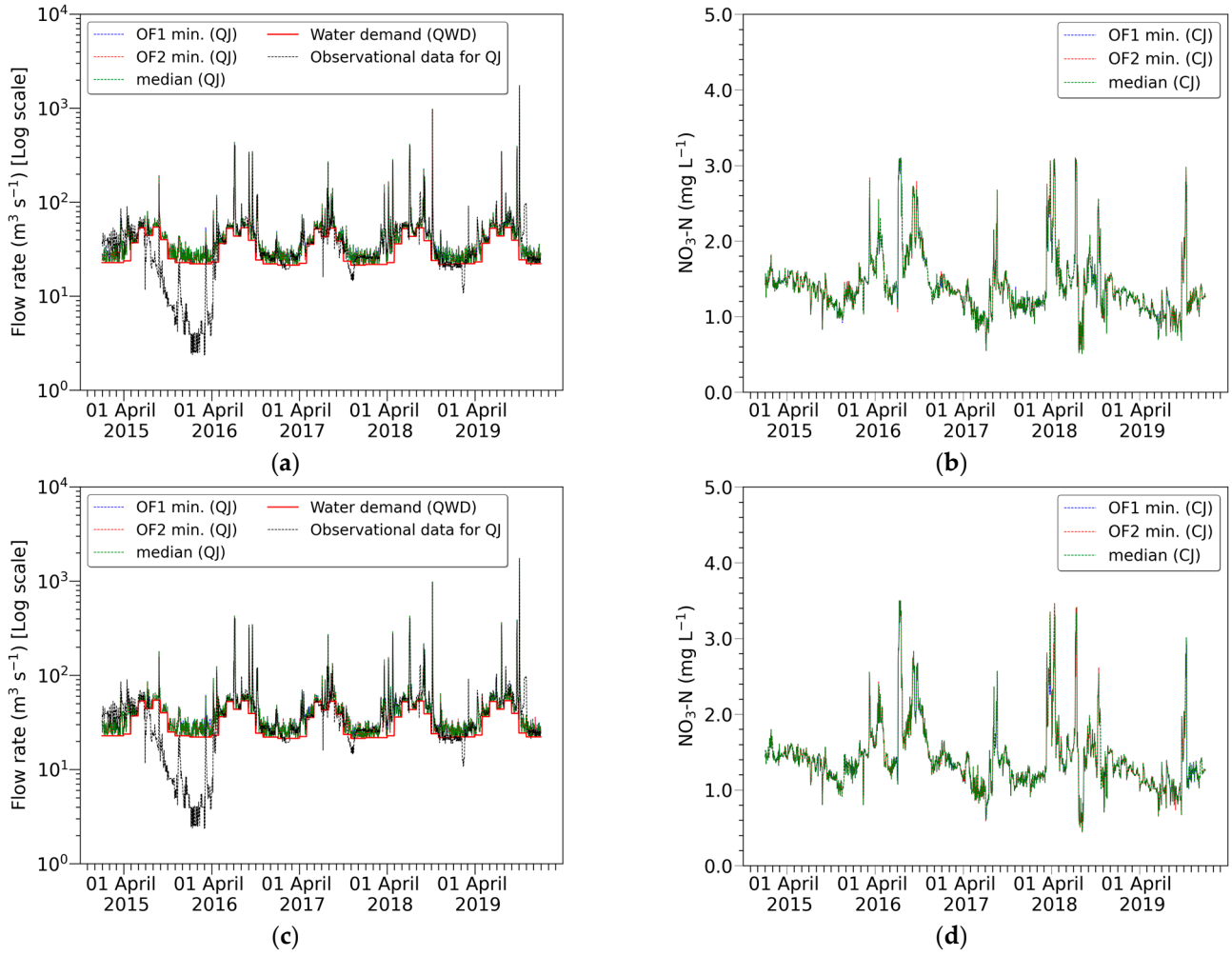


**Figure A3.** *Cont.*

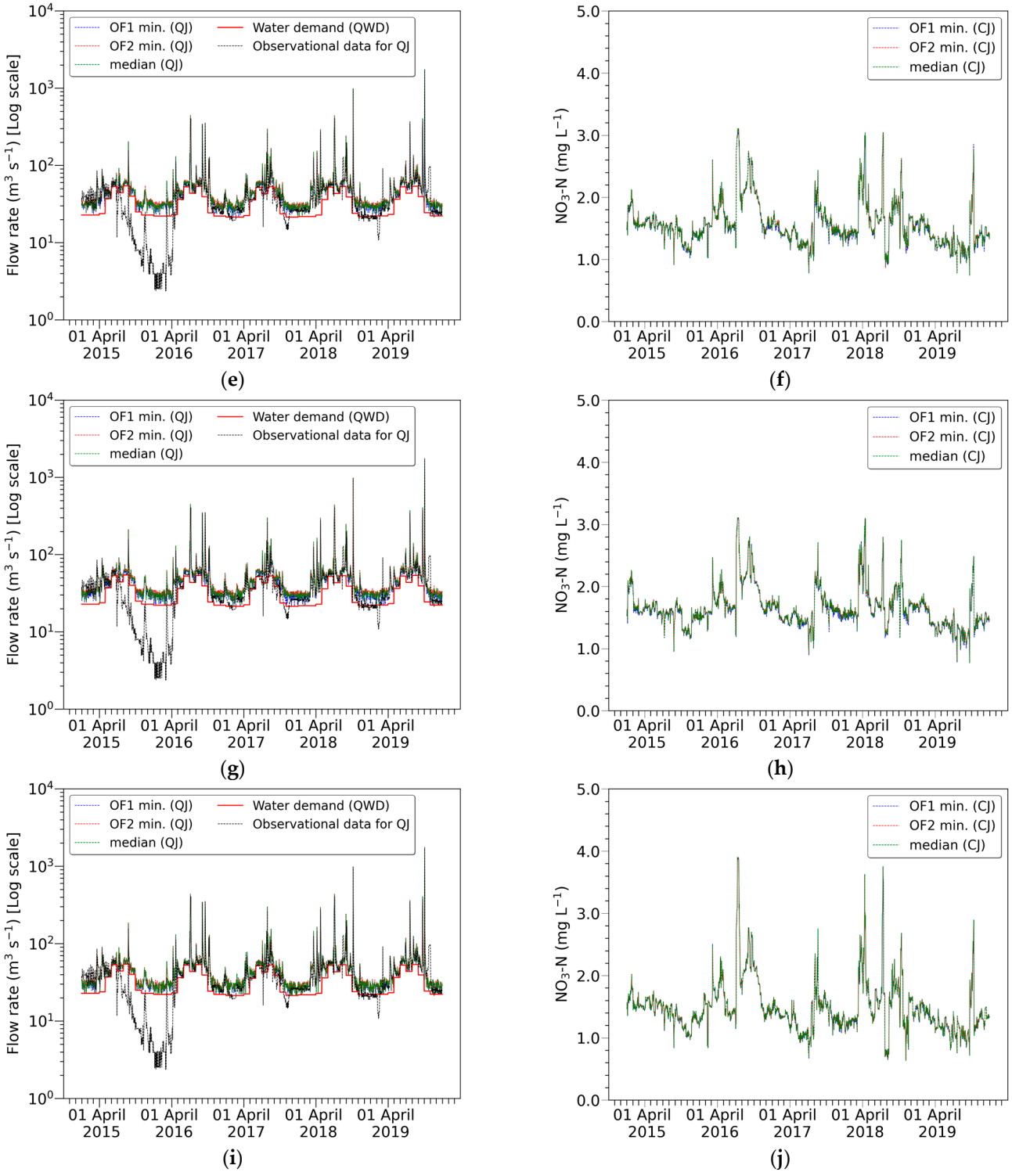


**Figure A3.** *Cont.*

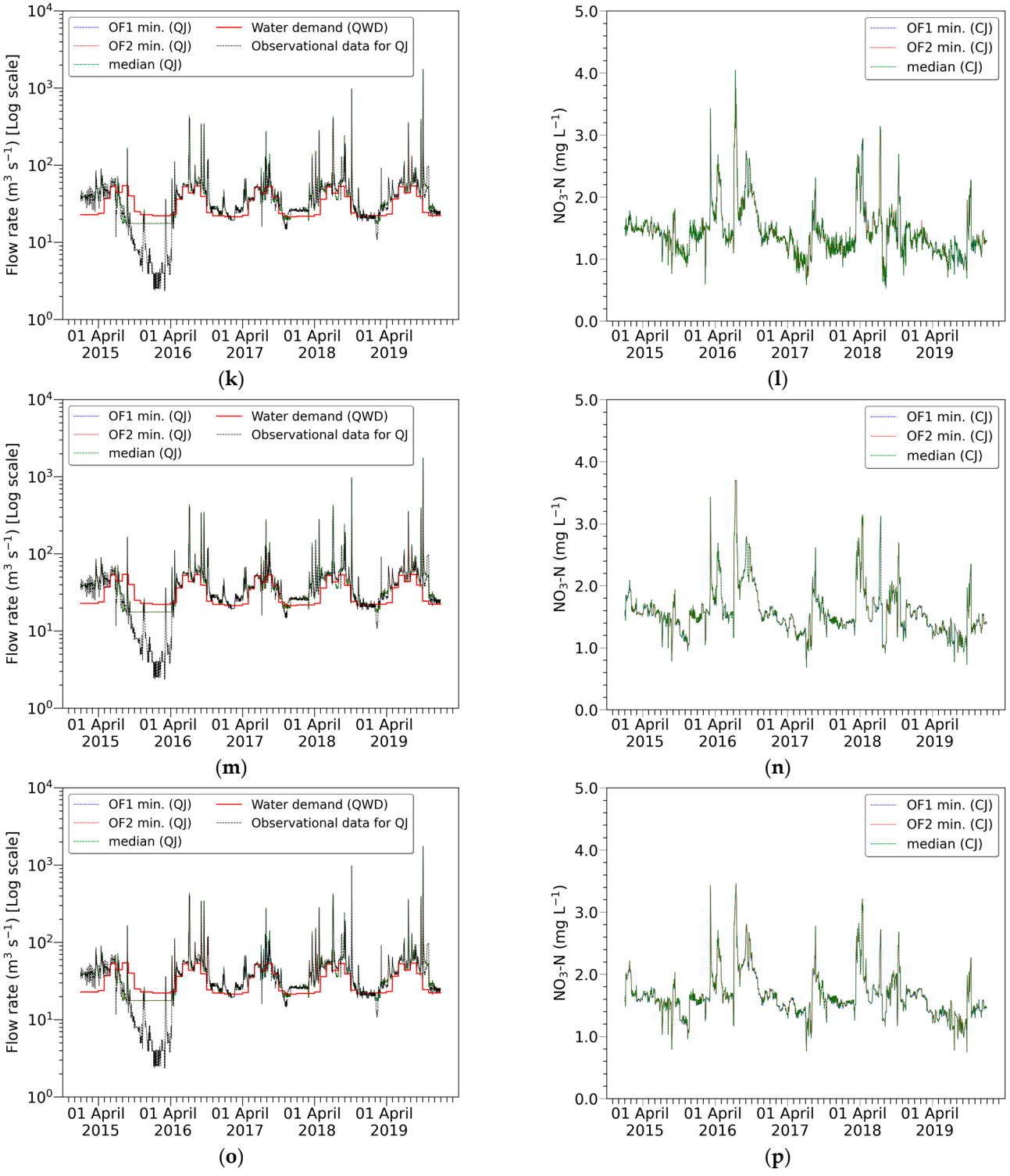


**Figure A3.** *Cont.*

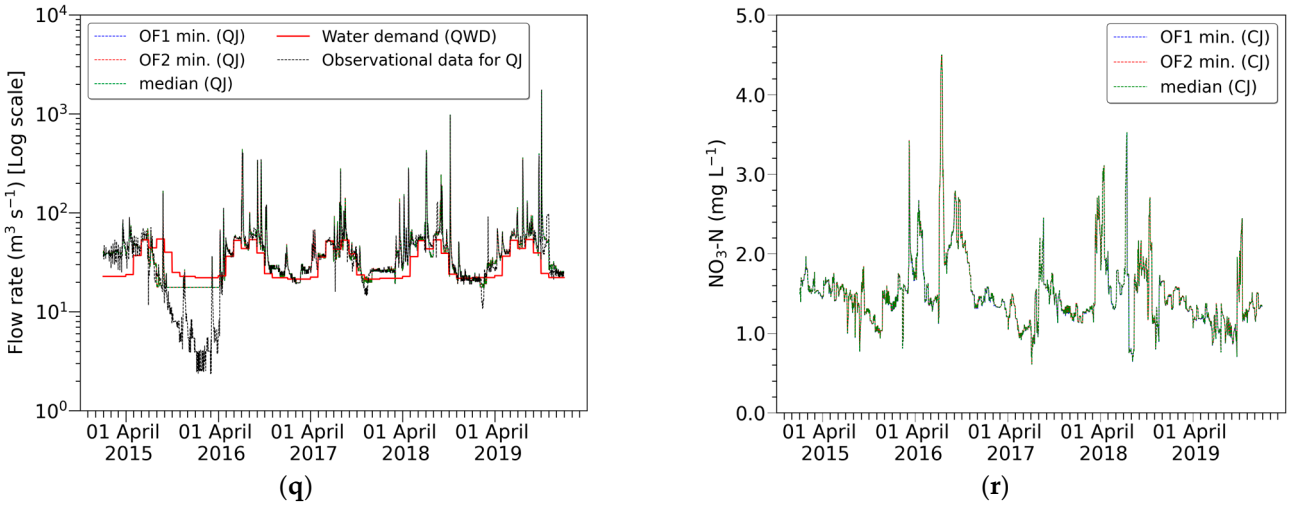


**Figure A3.** Optimization results (*QJ* and *CJ*) for three optimal solutions (OF1 min., OF2 min., and median): (**a**) *QJ* for Case 1; (**b**) *CJ* for Case 1; (**c**) *QJ* for Case 2; (**d**) *CJ* for Case 2; (**e**) *QJ* for Case 3; (**f**) *CJ* for Case 3; (**g**) *QJ* for Case 4; (**h**) *CJ* for Case 4; (**i**) *QJ* for Case 5; (**j**) *CJ* for Case 5; (**k**) *QJ* for Case 6; (**l**) *CJ* for Case 6; (**m**) *QJ* for Case 7; (**n**) *CJ* for Case 7; (**o**) *QJ* for Case 8; (**p**) *CJ* for Case 8; (**q**) *QJ* for Case 9; (**r**) *CJ* for Case 9.

## References

1. Yoo, J.-H. Maximization of Hydropower Generation through the Application of a Linear Programming Model. *J. Hydrol.* **2009**, *376*, 182–187. [CrossRef]
2. Saadatpour, M.; Javaheri, S.; Afshar, A.; Solis, S.S. Optimization of Selective Withdrawal Systems in Hydropower Reservoir Considering Water Quality and Quantity Aspects. *Expert Syst. Appl.* **2021**, *184*, 115474. [CrossRef]
3. Yosefipoor, P.; Saadatpour, M.; Solis, S.S.; Afshar, A. An Adaptive Surrogate-Based, Multi-Pollutant, and Multi-Objective Optimization for River-Reservoir System Management. *Ecol. Eng.* **2022**, *175*, 106487. [CrossRef]
4. Saadatpour, M.; Afshar, A.; Solis, S.S. Surrogate-Based Multiperiod, Multiobjective Reservoir Operation Optimization for Quality and Quantity Management. *J. Water Resour. Plan. Manag.* **2020**, *146*, 04020053. [CrossRef]
5. Modabberi, A.; Noori, R.; Madani, K.; Ehsani, A.H.; Mehr, A.D.; Hooshyaripor, F.; Klove, B. Caspian Sea is Eutrophying: The Alarming Message of Satellite Data. *Environ. Res. Lett.* **2020**, *15*, 124047. [CrossRef]
6. Jankowiak, J.; Hattenrath-Lehmann, T.; Kramer, B.J.; Ladds, M.; Gobler, C.J. Deciphering the Effects of Nitrogen, Phosphorus, and Temperature on Cyanobacterial Bloom Intensification, Diversity, and Toxicity in Western Lake Erie. *Limnol. Oceanogr.* **2019**, *64*, 1347–1370. [CrossRef]
7. Park, H.-K.; Lee, H.-J.; Heo, J.; Yun, J.-H.; Kim, Y.-J.; Kim, H.-M.; Hong, D.-G.; Lee, I.-J. Deciphering the Key Factors Determining Spatio-Temporal Heterogeneity of Cyanobacterial Bloom Dynamics in the Nakdong River with Consecutive Large Weirs. *Sci. Total Environ.* **2021**, *755*, 143079. [CrossRef]
8. Xu, H.; Paerl, H.W.; Qin, B.; Zhu, G.; Hall, N.S.; Wu, Y. Determining Critical Nutrient Thresholds Needed to Control Harmful Cyanobacterial Blooms in Eutrophic Lake Taihu, China. *Environ. Sci. Technol.* **2015**, *49*, 1051–1059. [CrossRef]
9. Zhao, C.S.; Shao, N.F.; Yang, S.T.; Ren, H.; Ge, Y.R.; Feng, P.; Dong, B.E.; Zhao, Y. Predicting Cyanobacteria Bloom Occurrence in Lakes and Reservoirs before Blooms Occur. *Sci. Total Environ.* **2019**, *670*, 837–848. [CrossRef] [PubMed]
10. Mozafari, Z.; Noori, R.; Siadatmousavi, S.M.; Afzalimehr, H.; Azizpour, J. Satellite-Based Monitoring of Eutrophication in the Earth's Largest Transboundary Lake. *Geohealth* **2023**, *7*, e2022GH000770. [CrossRef]
11. Park, Y.; Pyo, J.; Kwon, Y.S.; Cha, Y.; Lee, H.; Kang, T.; Cho, K.H. Evaluating Physico-Chemical Influences on Cyanobacterial Blooms Using Hyperspectral Images in Inland Water, Korea. *Water Res.* **2017**, *126*, 319–328. [CrossRef]
12. Song, H.; Lynch, M.J. Restoration of Nature or Special Interests? A Political Economy Analysis of the Four Major Rivers Restoration Project in South Korea. *Crit. Criminol.* **2018**, *26*, 251–270. [CrossRef]
13. National Institute of Environmental Research. Water Environment Information System. Available online: https://water.nier.go.kr (accessed on 24 April 2023).
14. Carmichael, W.W.; Boyer, G.L. Health Impacts from Cyanobacteria Harmful Algae Blooms: Implications for the North American Great Lakes. *Harmful Algae* **2016**, *54*, 194–212. [CrossRef] [PubMed]
15. Falconer, I.R.; Humpage, A.R. Health Risk Assessment of Cyanobacterial (Blue-Green Algal) Toxins in Drinking Water. *Int. J. Environ. Res. Public Health* **2005**, *2*, 43–50. [CrossRef]
16. Falconer, I.R. Is There a Human Health Hazard from Microcystins in the Drinking Water Supply? *Acta Hydrochim. Hydrobiol.* **2005**, *33*, 64–71. [CrossRef]

17. May, N.W.; Olson, N.E.; Panas, M.; Axson, J.L.; Tirella, P.S.; Kirpes, R.M.; Craig, R.L.; Gunsch, M.J.; China, S.; Laskin, A.; et al. Aerosol Emissions from Great Lakes Harmful Algal Blooms. *Environ. Sci. Technol.* **2018**, *52*, 397–405. [CrossRef]
18. Plaas, H.E.; Paerl, H.W. Toxic Cyanobacteria: A Growing Threat to Water and Air Quality. *Environ. Sci. Technol.* **2021**, *55*, 44–64. [CrossRef]
19. Rousso, B.Z.; Bertone, E.; Stewart, R.; Hamilton, D.P. A Systematic Literature Review of Forecasting and Predictive Models for Cyanobacteria Blooms in Freshwater Lakes. *Water Res.* **2020**, *182*, 115959. [CrossRef]
20. Ralston, D.K.; Moore, S.K. Modeling Harmful Algal Blooms in a Changing Climate. *Harmful Algae* **2020**, *91*, 101729. [CrossRef]
21. Qin, R.F.; Yang, S.; Xu, Z.A.; Hong, T.F. Development of a Web-Based Modelling Framework for Harmful Algal Blooms Transport Simulation Using Open-Source Technologies. *J. Environ. Manag.* **2023**, *325*, 116616. [CrossRef]
22. Kim, J.; Kwak, J.; Ahn, J.M.; Kim, H.; Jeon, J.; Kim, K. Oscillation Flow Dam Operation Method for Algal Bloom Mitigation. *Water* **2022**, *14*, 1315. [CrossRef]
23. Lee, D.Y.; Baek, K.O. Study of the Mitigation of Algae in Lake Uiam according to the Operation of the Chuncheon Dam and the Soyang Dam. *KSCE J. Civ. Environ. Eng. Res.* **2022**, *42*, 171–179. [CrossRef]
24. Kim, W.; Lee, J.; Kim, J.; Kim, S. Assessment of Water Supply Stability for Drought-Vulnerable Boryeong Multipurpose Dam in South Korea Using Future Dry Climate Change Scenarios. *Water* **2019**, *11*, 2403. [CrossRef]
25. Yu, J.S.; Shin, J.Y.; Kwon, M.; Kim, T.-W. Bivariate Drought Frequency Analysis to Evaluate Water Supply Capacity of Multi-Purpose Dams. *KSCE J. Civ. Environ. Eng. Res.* **2017**, *37*, 231–238. [CrossRef]
26. Yoo, C.; Jun, C.; Zhu, J.; Na, W. Evaluation of Dam Water-Supply Capacity in Korea Using the Water-Shortage Index. *Water* **2021**, *13*, 956. [CrossRef]
27. Kim, S.K.; Choi, S.-U. Assessment of the Impact of Selective Withdrawal on Downstream Fish Habitats Using a Coupled Hydrodynamic and Habitat Modeling. *J. Hydrol.* **2021**, *593*, 125665. [CrossRef]
28. Smith, D.R.; Wilhelms, S.C.; Holland, J.P.; Dortch, M.S.; Davis, J.E. *Improved Description of Selective Withdrawal through Point Sinks*; U.S. Army Corps of Engineers, Waterways Experiment Station: Vicksburg, MS, USA, 1987. Available online: https://erdc-library.erdc.dren.mil/jspui/handle/11681/4508 (accessed on 15 February 2023).
29. Davis, J.E.; Holland, J.P.; Schneider, M.L.; Wilhelms, S.C. *SELECT: A Numerical, One-Dimensional Model for Selective Withdrawal*; U.S. Army Corps of Engineers, Waterways Experiment Station: Vicksburg, MS, USA, 1987. Available online: https://erdc-library.erdc.dren.mil/jspui/handle/11681/4346 (accessed on 15 February 2023).
30. Bohan, J.P.; Grace, J.L. *Selective Withdrawal from Man-Made Lakes*; U.S. Army Corps of Engineers, Waterways Experiment Station: Vicksburg, MS, USA, 1973. Available online: https://erdc-library.erdc.dren.mil/jspui/handle/11681/13227 (accessed on 15 February 2023).
31. Lee, S.; Kim, J.; Noh, J.; Ko, I.H. Assessment of Selective Withdrawal Facility in the Imha Reservoir Using CE-QUAL-W2 Model. *J. Korean Soc. Water Environ.* **2007**, *23*, 228–235.
32. Kim, J.; Kim, H.Y.; Choi, H.G.; Jeong, S.; Lee, Y. The Innovative Operation of Imha Reservoir. *E3S Web Conf.* **2022**, *346*, 01029. [CrossRef]
33. Park, H.; Chung, S.; Cho, E.; Lim, K. Impact of Climate Change on the Persistent Turbidity Issue of a Large Dam Reservoir in the Temperate Monsoon Region. *Clim. Chang.* **2018**, *151*, 365–378. [CrossRef]
34. Lee, H.-J.; Park, H.-K.; Cheon, S.-U. Effects of Weir Construction on Phytoplankton Assemblages and Water Quality in a Large River System. *Int. J. Environ. Res. Public Health* **2018**, *15*, 2348. [CrossRef]
35. Elzain, H.E.; Chung, S.Y.; Senapathi, V.; Sekar, S.; Lee, S.Y.; Priyadarsi, R.D.; Hassan, A.; Sabarathinam, C. Comparative Study of Machine Learning Models for Evaluating Groundwater Vulnerability to Nitrate Contamination. *Ecotoxicol. Environ. Saf.* **2022**, *229*, 113061. [CrossRef] [PubMed]
36. Park, H.-S.; Chung, S.-W. Water Transportation and Stratification Modification in the Andong-Imha Linked Reservoirs System. *J. Korean Soc. Water Environ.* **2014**, *30*, 31–43. [CrossRef]
37. Lee, J.; Bae, S.; Lee, D.-R.; Seo, D. Transportation Modeling of Conservative Pollutant in a River with Weirs-The Nakdong River Case. *J. Korean Soc. Environ. Eng.* **2014**, *36*, 821–827. [CrossRef]
38. Kim, J.; Seo, D.; Jang, M.; Kim, J. Augmentation of Limited Input Data Using an Artificial Neural Network Method to Improve the Accuracy of Water Quality Modeling in a Large Lake. *J. Hydrol.* **2021**, *602*, 126817. [CrossRef]
39. James, R.T. Recalibration of the Lake Okeechobee Water Quality Model (LOWQM) to Extreme Hydro-Meteorological Events. *Ecol. Model.* **2016**, *325*, 71–83. [CrossRef]
40. McIntyre, N.R.; Wheater, H.S. A Tool for Risk-Based Management of Surface Water Quality. *Environ. Model. Softw.* **2004**, *19*, 1131–1140. [CrossRef]
41. Cullinan, V.I.; May, C.W.; Brandenberger, J.M.; Judd, C.; Johnston, R.K. *Development of an Empirical Water Quality Model for Stormwater Based on Watershed Land Use in Puget Sound*; Space and Naval Warfare Systems Center, Marine Environmental Support Office: Bremerton, WA, USA, 2007. Available online: https://apps.dtic.mil/sti/citations/ADA519147 (accessed on 23 September 2022).
42. Kim, J.; Jonoski, A.; Solomatine, D.P. A Classification-Based Machine Learning Approach to the Prediction of Cyanobacterial Blooms in Chilgok Weir, South Korea. *Water* **2022**, *14*, 542. [CrossRef]
43. Srivastava, A.; Ahn, C.-Y.; Asthana, R.K.; Lee, H.-G.; Oh, H.-M. Status, Alert System, and Prediction of Cyanobacterial Bloom in South Korea. *Biomed Res. Int.* **2015**, *2015*, 584696. [CrossRef]

44. Jain, C.K. Application of Chemical Mass Balance to Upstream Downstream River Monitoring Data. *J. Hydrol.* **1996**, *182*, 105–115. [CrossRef]
45. Jha, R.; Ojha, C.S.P.; Bhatia, K.K.S. Non-Point Source Pollution Estimation Using a Modified Approach. *Hydrol. Process.* **2007**, *21*, 1098–1105. [CrossRef]
46. Deb, K.; Pratap, A.; Agarwal, S.; Meyarivan, T. A Fast and Elitist Multiobjective Genetic Algorithm: NSGA-II. *IEEE Trans. Evol. Comput.* **2002**, *6*, 182–197. [CrossRef]
47. Blank, J.; Deb, K. Pymoo: Multi-Objective Optimization in Python. *IEEE Access* **2020**, *8*, 89497–89509. [CrossRef]
48. Kim, J.; Jonoski, A.; Solomatine, D.P.; Goethals, P.L.M. Water Quality Modelling for Nitrate Nitrogen Control Using HEC-RAS: Case Study of Nakdong River in South Korea. *Water* **2023**, *15*, 247. [CrossRef]
49. Brunner, G.W. *HEC-RAS River Analysis System User's Manual Version 5.0*; U.S. Army Corps of Engineers, Institute for Water Resources, Hydrologic Engineering Center: Davis, CA, USA, 2016. Available online: https://www.hec.usace.army.mil/software/hec-ras/documentation/HEC-RAS%205.0%20Users%20Manual.pdf (accessed on 20 January 2022).
50. Aguilar, J.; Van Andel, S.-J.; Werner, M.; Solomatine, D.P. Hydrodynamic and Water Quality Surrogate Modeling for Reservoir Operation. In Proceedings of the 11th International Conference on Hydroinformatics, New York, NY, USA, 17–21 August 2014.
51. Moriasi, D.N.; Gitau, M.W.; Pai, N.; Daggupati, P. Hydrologic and Water Quality Models: Performance Measures and Evaluation Criteria. *Trans. ASABE* **2015**, *58*, 1763–1785. [CrossRef]
52. Başağaoğlu, H.; Chakraborty, D.; Lago, C.D.; Gutierrez, L.; Şahinli, M.A.; Giacomoni, M.; Furl, C.; Mirchi, A.; Moriasi, D.; Şengör, S.S. A Review on Interpretable and Explainable Artificial Intelligence in Hydroclimatic Applications. *Water* **2022**, *14*, 1230. [CrossRef]
53. Paerl, H.W.; Otten, T.G. Harmful Cyanobacterial Blooms: Causes, Consequences, and Controls. *Microb. Ecol.* **2013**, *65*, 995–1010. [CrossRef] [PubMed]
54. Paerl, H.W.; Fulton, R.S.; Moisander, P.H.; Dyble, J. Harmful Freshwater Algal Blooms, with an Emphasis on Cyanobacteria. *Sci. World J.* **2001**, *1*, 76–113. [CrossRef]
55. Noori, R.; Ansari, E.; Jeong, Y.W.; Aradpour, S.; Maghrebi, M.; Hosseinzadeh, M.; Bateni, S.M. Hyper-Nutrient Enrichment Status in the Sabalan Lake, Iran. *Water* **2021**, *13*, 2874. [CrossRef]
56. Zakova, Z.; Berankova, D.; Kockova, E.; Kriz, P. Influence of Diffuse Pollution on the Eutrophication and Water-Quality of Reservoirs in the Morava River Basin. *Water Sci. Technol.* **1993**, *28*, 79–90. [CrossRef]
57. Harrow-Lyle, T.; Kirkwood, A.E. The Invasive Macrophyte Nitellopsis Obtusa May Facilitate the Invasive Mussel Dreissena Polymorpha and Microcystis Blooms in a Large, Shallow Lake. *Can. J. Fish. Aquat.* **2020**, *77*, 1201–1208. [CrossRef]
58. Deng, D.G.; Xie, P.; Zhou, Q.; Yang, H.; Guo, L.G. Studies on Temporal and Spatial Variations of Phytoplankton in Lake Chaohu. *J. Integr. Plant Biol.* **2007**, *49*, 409–418. [CrossRef]
59. Jahan, R.; Khan, S.; Haque, M.M.; Choi, J.K. Study of Harmful Algal Blooms in a Eutrophic Pond, Bangladesh. *Environ. Monit. Assess.* **2010**, *170*, 7–21. [CrossRef]
60. Yang, Y.; Chen, H.; Lu, J. Inactivation of Algae by Visible-Light-Driven Modified Photocatalysts: A Review. *Sci. Total Environ.* **2023**, *858*, 159640. [CrossRef] [PubMed]
61. Ustaoglu, F.; Tas, B.; Tepe, Y.; Topaldemir, H. Comprehensive Assessment of Water Quality and Associated Health Risk by Using Physicochemical Quality Indices and Multivariate Analysis in Terme River, Turkey. *Environ. Sci. Pollut. Res.* **2021**, *28*, 62736–62754. [CrossRef]
62. Forio, M.A.E.; Goethals, P.L.M. An Integrated Approach of Multi-Community Monitoring and Assessment of Aquatic Ecosystems to Support Sustainable Development. *Sustainability* **2020**, *12*, 5603. [CrossRef]
63. Gao, L.L.; Li, D.L. A Review of Hydrological/Water-Quality Models. *Front. Agric. Sci. Eng.* **2014**, *1*, 267–276. [CrossRef]
64. Goethals, P.L.M.; Forio, M.A.E. Advances in Ecological Water System Modeling: Integration and Leanification as a Basis for Application in Environmental Management. *Water* **2018**, *10*, 1216. [CrossRef]
65. Ho, L.; Goethals, P. Machine Learning Applications in River Research: Trends, Opportunities and Challenges. *Methods Ecol. Evol.* **2022**, *13*, 2603–2621. [CrossRef]
66. Chowdury, M.S.U.; Bin Emran, T.; Ghosh, S.; Pathak, A.; Alam, M.M.; Absar, N.; Andersson, K.; Hossain, M.S. IoT Based Real-time River Water Quality Monitoring System. *Procedia Comput. Sci.* **2019**, *155*, 161–168. [CrossRef]
67. Zeng, G.; Zhang, R.; Liang, D.; Wang, F.; Han, Y.; Luo, Y.; Gao, P.; Wang, Q.; Wang, Q.; Yu, C. Comparison of the Advantages and Disadvantages of Algae Removal Technology and Its Development Status. *Water* **2023**, *15*, 1104. [CrossRef]